Volcanic eruptions on mid-ocean ridges: New evidence from the superfast spreading East Pacific Rise, 17°–19°S

John Sinton,[1] Eric Bergmanis,[1] Ken Rubin,[1] Rodey Batiza,[1,2] Tracy K. P. Gregg,[3] Karl Grönvold,[4] Ken C. Macdonald,[5] and Scott M. White[6]

Received 6 December 2000; revised 25 November 2001; accepted 30 November 2001; published 14 June 2002.

[1] Side-scan sonar, submersible observations and sampling of lava flows from the East Pacific Rise, 17°–19°S constrain the character and variability of submarine volcanic eruptions along mid-ocean ridges. Nine separate lava sequences were mapped using relative age and lithological contrasts among recovered samples. Axial lengths activated during eruptive episodes range from ~1 to >18 km; individual flow field areas vary from <1 to >19 km^2. Estimated erupted volumes range from <1 to >200 × 10^6 m^3. The largest unit is the chemically uniform Animal Farm lava near 18°37′S. The youngest lava is the Aldo-Kihi flow field, 17°24′–34′S, probably erupted in the early 1990s from a fissure system extending >18 km along axis. Near 18°33′S two distinct lava compositions with uniform sediment cover were recovered from lava that buries older faulted terrain. The boundary in lava composition coincides with a change in depth to the top of an axial magma lens seismic reflector, consistent with magmas from two separate reservoirs being erupted in the same event. Chemical compositions from throughout the area indicate that lavas with identical compositions can be emplaced in separate volcanic eruptions within individual segments. A comparison of our results to global data on submarine mid-ocean ridge eruptions suggests consistent dependencies of erupted volume, activated fissure lengths, and chemical heterogeneity with spreading rate, consistent with expected eruptive characteristics from ridges with contrasting thermal properties and magma reservoir depths. *INDEX TERMS:* 3035 Marine Geology and Geophysics: Midocean ridge processes; 8414 Volcanology: Eruption mechanisms; 8439 Volcanology: Physics and chemistry of magma bodies; 3655 Mineralogy and Petrology: Major element composition; *KEYWORDS:* lava flow, chemical heterogeneity, erupted volume, lava morphology, side-scan sonar

1. Introduction

[2] The study of the products of individual volcanic eruptions is one of the most direct ways to assess the nature of the magma reservoirs that feed them, as well as the plumbing system that delivers magma to the surface. For example, the volumes and chemical composition of individual lava flows provide constraints on the size, temperature, and internal variation within subvolcanic magma reservoirs. At mid-ocean ridges the along-axis limit of eruptive fissures can be used to infer aspects of the magma transport processes during eruptions, and lava morphology can be used to address local flow velocities and effusion rates. The size and age of individual eruptions constrain recurrence intervals and eruptive frequencies for individual ridge segments.

[3] Despite these obvious motivations, few individual lava flows have been mapped on mid-ocean ridges outside of Iceland (see *Perfit and Chadwick* [1998] for a review). This partly reflects a paucity of geological observations on the seafloor at the scale of individual lava flows. *Ballard and van Andel* [1977] provided some of the first volcanological data on seafloor volcanic edifices through the delineation of flow directions and vent structures in the FAMOUS area along the Mid-Atlantic Ridge near 37°N. Since then, relatively few detailed data became available until the early 1990s, with detailed work on recent lava flows on the intermediate spreading (50–60 mm/yr) Juan de Fuca and Gorda Ridges [*Chadwick and Embley*, 1994; *Chadwick et al.*, 1991, 1995, 1998; *Embley and Chadwick*, 1994; *Embley et al.*, 1991, 2000; *Smith et al.*, 1994; *Rubin et al.*, 1998; *Smith*, 1999], the advent of near-real-time seismic monitoring of NE Pacific spreading centers [*Fox et al.*, 1994] and the discovery and documentation of a recent eruption near 9°50′N on the East Pacific Rise [*Haymon et al.*, 1993; *Rubin et al.*, 1994; *Gregg et al.*, 1996].

[4] The results of the French-American Nautile Dorsale Ultra-Rapide (NAUDUR) program of 1993 [*Auzende et al.*,

[1]Department of Geology and Geophysics, University of Hawaii at Manoa, Honolulu, Hawaii, USA.
[2]Now at National Science Foundation, Division of Ocean Sciences, Arlington, Virginia, USA.
[3]Department of Geological Sciences, University at Buffalo, Buffalo, New York, USA.
[4]Nordic Volcanological Institute, Reykjavík, Iceland.
[5]Department of Geological Sciences, University of California, Santa Barbara, California, USA.
[6]Department of Geological Sciences, University of South Carolina, Columbia, South Carolina, USA.

0148-0227/02/2000JB000090$09.00

1994, 1996] indicated that the southern East Pacific Rise, between 17° and 19°S is an ideal place to investigate eruptive processes at the high end of the spreading rate spectrum. Auzende et al. described evidence for recent volcanism in the area, as well as contacts between various lava flows of differing ages. However, individual lava flows were not completely mapped during that reconnaissance expedition, so critical information on the lengths of ridge axis activated during single events and lava flow areas, volumes, and morphological variations was incomplete for those units encountered. Analyses of NAUDUR samples gave preliminary estimates of the range of chemical variability within some eruptive units, but this aspect and its significance also remained to be better documented by future study.

[5] In this paper we report the results of a 1999 investigation of eruptive units along the East Pacific Rise axis between 17° and 19°S, where spreading rates are ~145 mm/yr [*Naar and Hey*, 1989]. The objectives of this investigation were to constrain erupted volumes, fissure lengths, lava flow morphology, and internal chemical heterogeneity, as indicators of subaxial magma reservoirs and eruptive processes occurring in this region. We used data from a deep-towed, 120-kHz side-scan sonar and bathymetric mapping system, submersible dives, and extensive sample collections to completely map and characterize seven distinct lava fields in this area. Several other flows were sampled and partially mapped. The results reported here nearly double the number of well-studied submarine lava flows [*Perfit and Chadwick*, 1998] and extend the mid-ocean ridge lava flow catalogue to superfast spreading rates.

1.1. Deciphering the Products of Submarine Eruptions

[6] There is little information on the details of mid-ocean ridge eruptions outside of Iceland. Some Icelandic eruptions appear to be associated with major rifting episodes involving inflow of magma into crustal magma chambers and rifting of the plate boundary [*Bjornsson*, 1985; *Einarsson*, 1991]. A primary feature of rifting in north Iceland is that it is episodic. Individual fault/fissure swarms may rest for a few thousand years, while others may become active, one at the time, on timescales of a century or more. The 9-year, 1975–1984, Krafla episode involved ~20 rifting/magmatic events, each lasting from a few hours to 2 weeks. During the first half of the Krafla episode, different segments of the 100-km-long Krafla fault swarm rifted up to 3 m in each event. The few eruptions that accompanied this early phase were small, but the underground movement of magma could be monitored by inflation and deflation of magma reservoirs located at a depth of ~3 km below the center of the Krafla central volcano. During the second half of the episode all the events were accompanied by lava eruptions. The total volume of the nine individual eruptions is ~0.25 km^3, which is only about a third of the volume of magma inferred from the inflation/deflation cycles to have moved through the central magma chamber(s). Although the total length of the Krafla fissure swarm that eventually rifted was over 60 km, the maximum length of the eruptive fissures was just over 8 km in length. Each of the eruptive events associated with the Krafla episode produced several different lava flows that were mapped separately by contemporary observers [*Saemundsson*, 1991]. However, an observer without the real-time observations would not be able to distinguish individual lava flows of this episode, although the Krafla lavas are easily distinguished from the next previous rifting/eruption episode of the fault swarm, the Mývatn Fires of 1724–1729.

[7] The Krafla Fires were the latest of five rifting episodes occurring in this region over the last 2800 years. These five episodes are collectively referred to as the Hverfjall period, which was the second major period of rifting in this part of Iceland in postglacial time. The previous rifting period (Lúdent period) ended ~7500 years ago [*Saemundsson*, 1991]. Thus, in the case of north Iceland, one can define a hierarchy of eruptive phenomena that range from individual lava flows produced from separate eruptions (eruptive events) that together constitute rifting episodes and so on. Each eruptive event produced one or more individual lava flows, and the entire assemblage of the Krafla Fires constitutes a lava flow field.

[8] Whether or not submarine mid-ocean ridge eruptions also occur in "periods" encompassing multiple "episodes," which in turn consist of several closely spaced "events" is generally unknown, although evidence from 9°50′N [*Rubin et al.*, 1994] indicates that there were separate eruptions in this area in both 1991 and 1992. As noted above, although the products of individual events of the Krafla Fires are difficult to impossible to map today, the contrast between the Krafla episode lavas flow field and the surrounding terrain, representing more than 200 years, is much more striking and can be identified and mapped with confidence.

[9] Various techniques can be employed in mapping submarine lava sequences. Perhaps the most reliable is visual observations of contrasting age on the seafloor. *Chadwick et al.* [1998] employed this technique to confirm recent eruptive products that were first detected by seismicity swarms. Another technique involves the documentation of morphological changes determined from repeat bathymetric surveys [*Chadwick et al.*, 1995; *Embley et al.*, 2000]. The accuracy of such interpretations depends, of course, on the precision and resolution of the survey data. *Macdonald et al.* [1989] and *Edwards et al.* [2001] used contrasting side-scan sonar reflectivity to determine the areas of large lava flow fields close to the East Pacific Rise (EPR) near 8°S and along the Gakkel Ridge, respectively. Cursory sampling of the EPR 8°S flow field [*Hall and Sinton*, 1996] indicated a range of chemical compositions, and *Hall and Sinton* [1996] suggested that the field was produced by more than one eruption. However, this result highlights an additional uncertainty in the study of submarine eruptions, namely the chemical heterogeneity of single eruptive events and episodes. Although chemical mapping [e.g., *Reynolds et al.*, 1992] provides a way to assess aspects of the spatial and temporal diversity within a region, it might provide little information on the scales of single eruptive events if the products from those events are chemically heterogeneous or if other events occurring in the same region have produced lavas that are chemically indistinguishable.

[10] Taken together, the most reliable approach to deciphering the products of single eruptive episodes appears to be geological observations of age and/or lithological contrast and superposition. It is worth emphasizing that prior to this study, it was generally unknown whether or not eruptions at superfast spreading can be separated into distinct episodes. As the period between eruptions decreases, the distinction

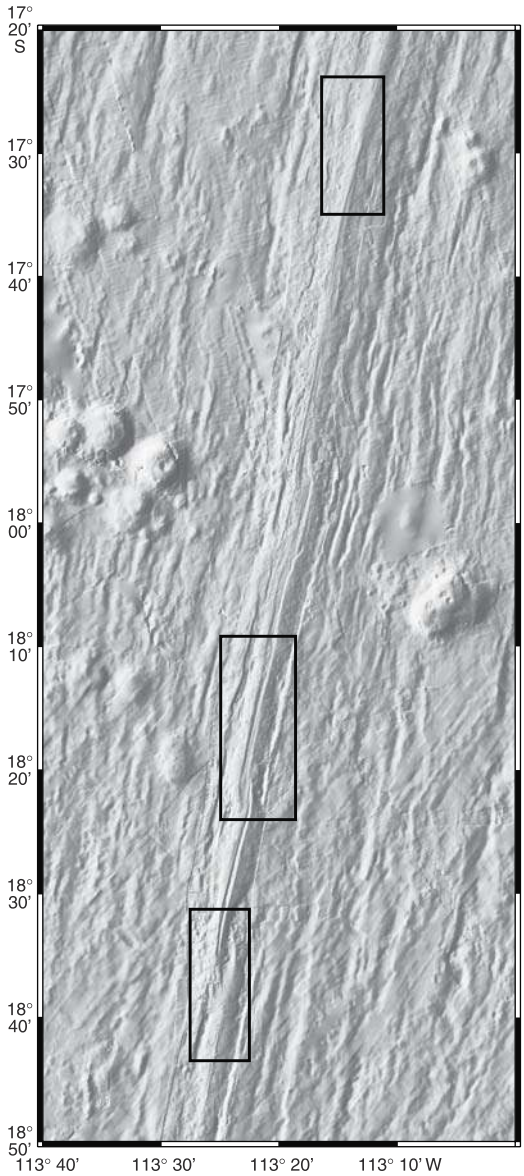

Figure 1. Shaded-relief map of the southern East Pacific Rise. Boxes denote the study areas referred to in this paper. Base map is from data of *Scheirer et al.* [1996].

between events and episodes obviously becomes blurred. In this study we used visual, video, and side-scan sonar observations to map age contrasts (contacts) on the seafloor and hence to define the products of individual eruptive episodes, which we refer to in this paper as lava flow fields. We sampled extensively in the study regions both to assess the extent of chemical heterogeneity within identified flow fields and to determine if the mapped units are chemically unique within the region. Flow field areas were calculated from the mapped outlines; thicknesses were constrained by observations at flow contacts and the depths of internal collapse structures.

1.2. East Pacific Rise 17°–19°S

[11] The East Pacific Rise (EPR) between 17° and 19°S shows a relatively wide range of axial morphologies and depths. Near 17°26′S the axis rises to its shallowest depth (<2590 m) south of the Garrett Fracture Zone. In cross-axis profiles the axial region has a domical shape. Southward from this point the axis continues to be an axial dome that deepens progressively. Locally, the summit is cut by an axial trough, typically <15 m deep and 30 m wide. The segment between 17°55′S and 18°08′S is an asymmetric half graben with the eastern flank rising more than 100 m above the graben floor. Between 18°08′S and 18°22′S the axial region is a graben that is ~250–600 m wide. The segment between 18°22′S and 18°37′S is a narrow, asymmetric graben that locally is <50 m wide. Farther to the south, the axis again has a dome shape but here rises only to ~2700 m depth. Thus the northernmost and southernmost segments both have axial domes, interpreted by *Macdonald and Fox* [1988], *Scheirer and Macdonald* [1993], *Auzende et al.* [1996], and *White et al.* [2000] as regions dominated by recent volcanic activity. In contrast, the intervening segments show evidence of significant faulting, rifting, and collapse [*Lagabrielle and Cormier*, 1999].

[12] We conducted high-resolution surveys and sampling in three principal areas along the EPR (Figure 1). The northernmost area includes the most inflated part of the ridge axis between the Garrett Fracture Zone and the Easter Microplate. It is the region where the Mantle Electromagnetic and Tomographic (MELT) experiment was conducted [*MELT Seismic Team*, 1998] and where *Auzende et al.* [1996] identified very recent volcanism. The middle region covers one of the rifted segments, whereas the southernmost area includes both the northern part of the inflated segment south of 18°37′S as well as the southern part of the highly tectonized Hump segment to the north. The following sections describe volcanic features of these regions, with special reference to nine newly mapped, volcanic units. A web site containing more detailed information on at-sea operations and sample descriptions from the STOWA cruise can be found at http://www.soest.hawaii.edu/STOWA.

[13] One of the features that makes these portions of the southern EPR ideal for volcanological investigation is a high sedimentation rate, variably estimated to be between 2 and 30 cm per1000 years [*Marchig et al.*, 1986; *Lyle et al.*, 1987; *Dekov and Kuptsov*, 1990, 1994]. The majority of lava flows lying >1 km off axis show significant sediment cover. However, there are many contributions to sedimentation, including local, hydrothermal sedimentation, and sediment redistribution, in addition to background abyssal sedimentation. Thus, although it is difficult to quantify lava flow ages based on sediment cover alone, our observations suggest that lava flows lying close to the axis that differ in age by tens to hundreds of years can be easily distinguished based on sediment cover. We used this feature, in addition to a variety of other standard geological techniques, to map lava flows of varying ages throughout the study area.

2. Observations

2.1. Animal Farm

[14] Work in the area between 18°35′S and 18°40′S was concentrated on a study of the Animal Farm lava flow field (Table 1), first discovered during the NAUDUR program [*Auzende et al.*, 1994]. Sheet flows dominate this unit, but it shows a range of lava morphologies, covering an area of

Table 1. Southern EPR Lava Flows

Event	Length, km	Area, km^2	Volume, $\times 10^6$ m^3	Comments
Animal Farm	13.3	18.5	220	mainly sheet lava; some pillow and lobate
Aldo-Kihi	18.5	14	140	1987–1993 eruption; mainly lobate
Moai	5.5	3.3	26	sheet lava with some lobate/pillow
Lava shield	1.9	1.06	12	pillow mound with summit crater
South Hump	5.5	0.89	7	lobate and sheet lava; postgraben
Buddha Flow	3.1	0.8	2	young lobate lava
Pillow mounds	~1.0	0.1–0.2	0.6–0.8	small, postgraben pillow mounds
Rehu-Marka	?	?	?	FeTi basalt; sheet and lobate flows
Next oldest flow	>13	?	?	mainly pillow and lobate lava

~18.5 km^2 (Figure 2 and Table 1). We estimate the average thickness of this unit, including possible subsurface void spaces, to be between 5 and 20 m, yielding a total volume of ~220 $\times$ 10^6 m^3. A series of right-stepping fissure swarms that mark the eruptive vents were mapped using the Deep Submergence Laboratory (DSL) 120-kHz side-scan sonar data and observations made from the Deep Submergence Vehicle *Alvin* along 13 km of ridge axis. South of 18°38′S these fissures occur just slightly to the eastern side of the topographic axial high and most of the lava flowed off axis to the east. In contrast, between 18°38′S and 18°36.5′S, the fissures lie on the west side of the topographic axis, and most of the lava was delivered to the west flank of the ridge. Lava distribution near the central part of the field mainly was accomplished through a series of anastomosing lava channels (Figure 3); the channels typically have lineated sheet flow floors that are bounded by folded sheet flow or lobate lava levees. Such features occur both within the axial fissures and radiating outward from the axis, particularly on the west flank. Near the distal ends of the sheet flows they typically become lobate or pillowed. The dominant lava morphology between 18°36′S and 18°35′S is lobate lava; lavas along the northernmost 3 km of the axis north of 18°35′S produced pillow mounds ~10–20 m high (Figure 3). These relations suggest that effusion rate progressively decreased northward from the center of the flow near 18°37′S, where the flow is widest. The limits of the Animal Farm lava are constrained by a number of *Alvin* crossings; the maximum distance the lava flowed away from the axis appears to be <2 km.

[15] The Animal Farm flow field is lightly dusted with sediment, which only locally is beginning to coalesce into small sediment pockets. We suspect that this amount of sediment cover corresponds to no more than 100 years in age in this area, as generally confirmed by a paleointensity age of 85 ± 35 years [*Carlut and Kent*, 2000] for several samples from the northern part of the flow field. However, in 1993 the low-temperature hydrothermal site near 18°37.5′S, 113°24′W, for which the lava flow field is named, was vigorously active, with widespread occurrence of thriving mussel beds, gastropods, fishes, and other organisms. Enteropneusts ("spaghetti worms") were not observed in the one dive that visited this area in 1993. When visited in 1999, the Animal Farm site apparently had cooled considerably, most of the bivalve community appeared to be dead or dying, and Enteropneusts were widespread along the eruptive fissures of the Animal Farm flow field. Thus, despite an apparent age more than 50 years, there appears to have been substantial changes in the low-temperature hydrothermal field between 1993 and 1999.

[16] Dive 3350 (Figure 2) traversed nearly unsedimented lobate lava that contains at least one vigorously venting, high-temperature "black smoker" hydrothermal vent site near 18°41′S, 113°25′W. The western boundary of this flow, called the Buddha Flow [*Sinton et al.*, 1999], shows a strong sedimentation contrast with older lava to the west. Its eastern contact with Animal Farm lava also is marked by an increase of sediment on the older lava; both the Animal Farm and Buddha lavas have lobate morphology in this region so the sediment contrast cannot be ascribed to different surface textures.

[17] Major element analyses of natural glasses from the area are shown in Figure 4. Fifty-five glass samples of the Animal Farm lava span a limited range of MgO contents between 7.2 and 7.4 wt %. Variation of most elements is only slightly greater than analytical uncertainty. Thus, the Animal Farm lava represents an exceedingly homogeneous eruption. The Buddha Flow is chemically identical to Animal Farm and the five analyzed samples are invariant within analytical precision (Table 2). The next oldest lava unit (Figure 2, Table 1) in the region contrasts in being mainly lobate lava with slightly greater sediment cover than Animal Farm; samples from this unit span a slightly greater range of chemical variability but at distinctly higher MgO contents. Although the Animal Farm magma has lower MgO than the next oldest lava in the area, modeling using the MELTS program [*Ghiorso and Sack*, 1995] suggests that the Animal Farm magma is derived from a parental magma with higher CaO and lower Na_2O (Figure 4), similar to even older lavas in the segment.

[18] It is notable that the compositional break between Animal Farm and the next oldest lava occurs across a sediment contrast that is so low in some places that the contact was identified only after reviewing dive tapes and processed side-scan sonar images. These contact relations suggest that the intervening period between the emplacement of the two units is unlikely to have been more than a few years to decades. Contact relations bounding the Buddha Flow were more distinct, possibly suggesting that the age contrast between it and Animal Farm is greater than between Animal Farm and the next oldest flow. However, there is a clear compositional difference between the next oldest flow and Animal Farm, a difference that is best explained by a mantle recharge event to have occurred in the intervening period, whereas Animal Farm and Buddha Flow are chemically identical. Taken together, we have evidence for at least three, closely spaced eruptive events

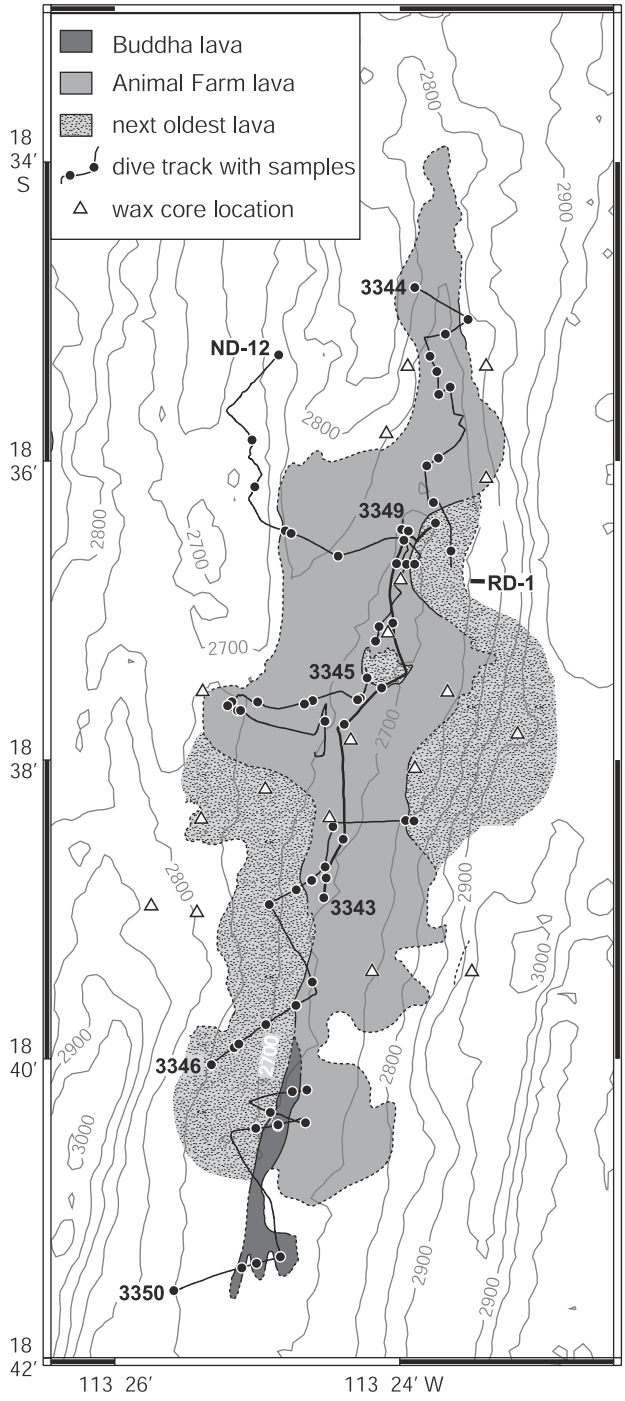

Figure 2. Map of the region around Animal Farm, showing boundaries of principal eruptive units, submersible dive tracks, and all sample locations. Shading shows different lava units (darkest is youngest).

having occurred in this segment, with the first two apparently separated by a mantle recharge event. These relations indicate a high frequency of magmatic events in this segment, consistent with its inflated morphology.

2.2. South Hump

[19] During NAUDUR dive 11 [*Auzende et al.*, 1996], relatively young lava near 18°33′S was seen to fill the axial graben and to be ponded against talus on the east wall. In places near the eastern margin of the flow, warm water appeared to be rising directly from the flow surface and a temperature anomaly of 2.5°C was measured 2–3 m above the flow surface [*Auzende et al.*, 1994]. These observations suggested that this lava might have been very recently emplaced. However, there was a nearly continuous, fine dusting of sediment over most of it. To constrain the spatial limits, age, and geochemical variability of young lava in this region, two *Alvin* dives were used in our 1999 program (Figure 5). We detected no temperature anomalies in 1999, and a fairly continuous coating of sediment was seen to cover flat-lying sheet flow surfaces, although small pockets of sediment had accumulated on pillow flows with higher local relief. The sediment cover is somewhat greater than on Animal Farm, possibly suggesting that the South Hump lava is older. Lavas with composition essentially identical to those collected on dive ND-11 and *Alvin* dive 3347 were also dredged from the axis in 1987 [*Sinton et al.*, 1991].

[20] A variety of geologic observations were used to constrain lava area, thickness, and morphology here. DSL 120-kHz side-scan sonar data and observations from *Alvin* in this region suggest that the South Hump lava extends as far south as 18°34.5′S and is essentially unfaulted, in contrast to the heavily faulted surrounding seafloor (Figure 5). The northern boundary of this unit is less clear on the 120-kHz sonar records, but relatively unfaulted lava appears to extend as far north as 18°31′S. The southern limit of young lava was constrained during *Alvin* dive 3347, which traversed northward to overlap with coverage of NAUDUR dive 11. *Alvin* dive 3348 crossed the northern contact of young lava near 18°31.5′S, where the flow front is a ramp of sheet lava that rises 4 m above the surrounding seafloor over ~5 m distance. The lavas beneath the South Hump flow field are heavily faulted lobate lavas. Further confirmation for a minimum thickness of 4 m at the northern end is derived from the fact that the flow buries a 4-m-high fault scarp in this region. To the south of the flow front the lava surface gradually rises an additional 33 m and changes from a sheet flow to lobate lava, locally mixed with pillow lava. Most likely the sheet lava flow front formed by slowly moving lava that oozed out from beneath a chilled roof, analogous to the formation of toothpaste lava in Hawaiian volcanoes [*Rowland and Walker*, 1987] and some submarine lineated sheet flows [*Chadwick et al.*, 1999].

[21] The chemical compositions of rocks recovered from the South Hump lava region are distinctly bimodal. Those from dives 3347 and ND-11 are highly evolved ferrobasalts with MgO <6.2 wt % and Na_2O contents <3.1 wt %. In contrast, samples collected during *Alvin* dive 3348 are basalts with ~7.2 wt % MgO and Na_2O contents >3.1 wt % (Figure 6). It is notable that no reasonable fractionation process predicts a decrease in Na with decreasing MgO over the range observed. Thus, not only are the two compositions from this region very different, but they cannot be related to one another by fractionation of the same parental magma.

[22] The boundary between the two chemical types was not crossed by any of the three dives in this area, indicating that it occurs between the northern limit of dive ND-11 and the southern limit of *Alvin* dive 3348 (Figure 7). However,

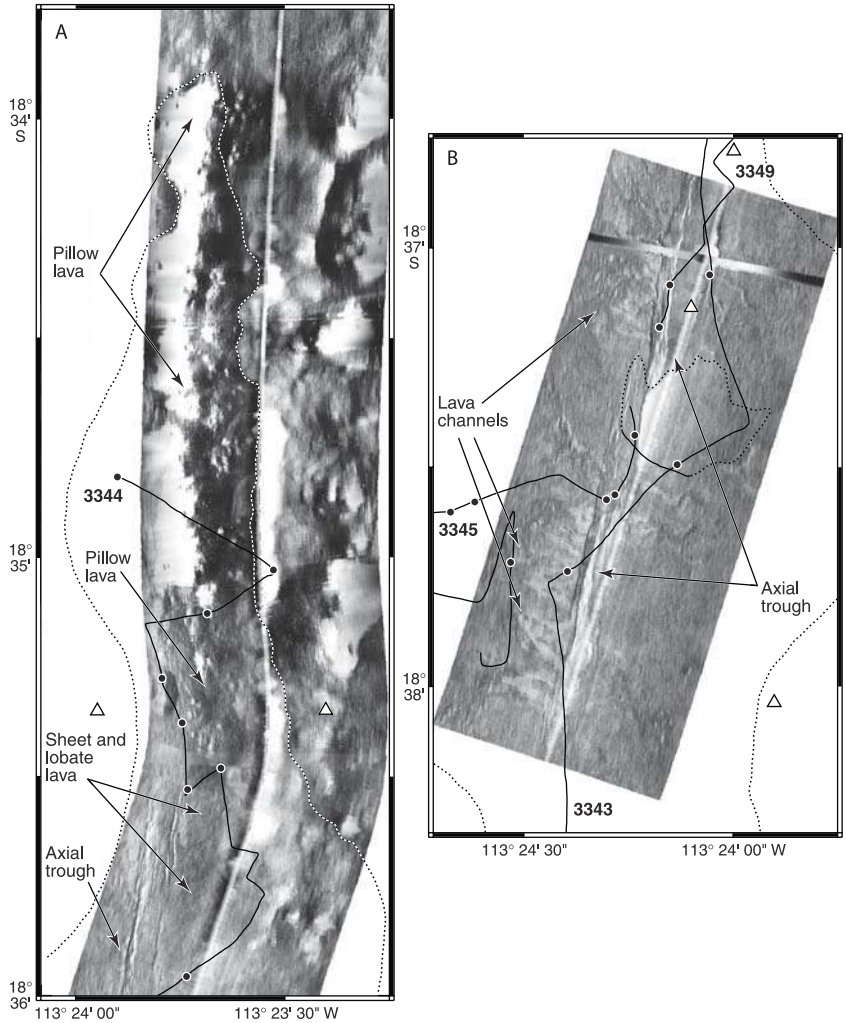

Figure 3. DSL 120-kHz side-scan sonar images of parts of the Animal Farm flow field. (a) Northern end of Animal Farm lava showing transition from lobate and sheet flows in the south to pillow mounds in the north. (b) Animal Farm lava near 18°38′S showing lava channels trending away from the axial trough.

there are no discernible boundaries on the side-scan sonar images in this region, and both areas show similar lack of faulting relative to the surrounding seafloor; dive observations suggest similar sediment cover in all places. Geological evidence therefore indicates that the entire axial graben between 18°31.5′S and 18°34.5′S was resurfaced either by a single, chemically bimodal eruption or by two adjacent eruptions that must have been close in age. In either case, the vastly different chemical compositions recovered have important implications for the nature of the subvolcanic reservoirs present in this region.

[23] The apparent boundary between the two chemical types coincides exactly with discontinuities in the axial magma chamber imaged by seismic reflection, as well as with significant differences in the thickness of seismic layer 2A [*Detrick et al.*, 1993; *Hooft et al.*, 1997] (Figure 7). Two magmas with different compositions, apparently residing in two separate magma reservoirs, have relatively recently been tapped, either during a single eruption or during closely spaced eruptions in adjacent regions. If all this lava represents the products of a single eruption, it suggests that the two reservoirs were not truly independent but rather possessed a mechanical and/or hydraulic (magmadraulic) connection. Such an occurrence is not unprecedented, in that bimodal eruption is also a characteristic of the Krafla Fires [*Grönvold and Mäkkipä*, 1978; *Grönvold*, 1984], with the two erupted chemical types spatially separated during single eruptions [*Einarsson*, 1991].

2.3. Intragraben Eruptions, 18°08′–18°22′S

[24] The axial region for this segment consists of an asymmetric graben, ~250–600 m wide. The western flank locally rises to <2650 m, ~50 m higher than the eastern flank (Figure 8). The graben walls consist of normal faults with individual scarps as high as 20 m. Six new *Alvin* dives, in addition to previous NAUDUR dives conducted in this region, indicate that the graben floor is intensely tectonized into horst and graben structures. Local collapses reveal lava lake structures with abundant lava pillars. Extensive fields of extinct hydrothermal chimneys are associated with the collapse zones. Elsewhere in the graben are younger lava flows that appear to drape preexisting structures.

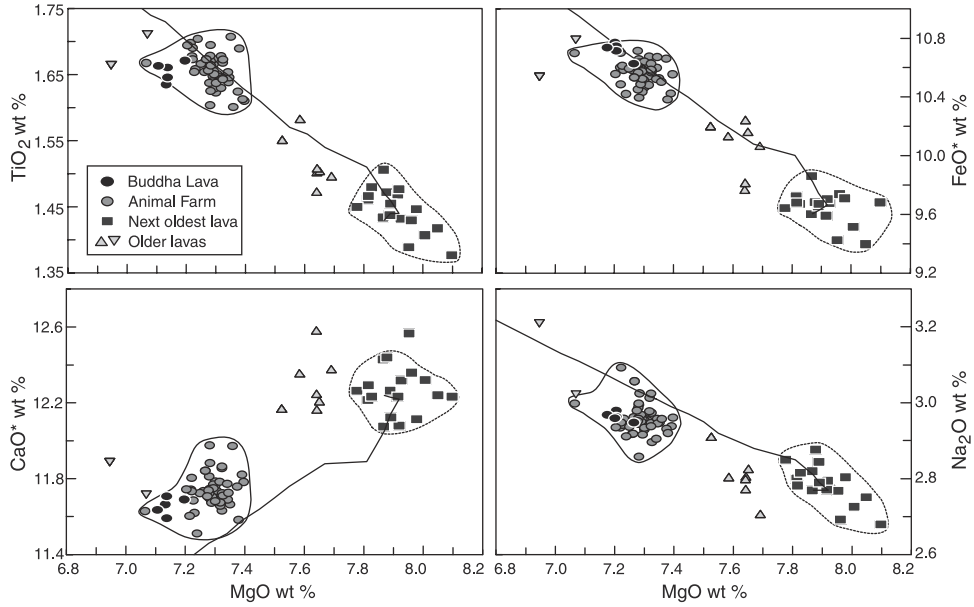

Figure 4. Chemical variations of lavas from the Animal Farm area. Solid line shows the fractionation trend at 500 bars calculated with the MELTS program [*Ghiorso and Sack*, 1995], using the mean composition of the next oldest lava with 0.3 wt % H_2O as the parent magma. Although some chemical variations suggest that the Animal Farm and next oldest lava could be related by low-pressure fractionation (e.g., TiO_2), the model fails to account for Na_2O and especially CaO variations. MELTS simulations at higher pressures and other water contents give even worse fits to the data. These results indicate that the magmas that were parental to the Animal Farm and next oldest lavas were chemically distinct, most likely requiring a mantle recharge event to have occurred in the period between these two eruptions. Buddha Flow lava samples plot within the field defined by Animal Farm samples for all elements.

[25] Some individual lava flow fields that clearly cut earlier structures are shown in Figure 8. The largest of these, named the Moai flow field because of the resemblance of the near-vent area in plan view to the famous statues of Easter Island, has an eruptive center near 18°10.5′S, where a well-developed channel system delivered a jumbled sheet flow, at least locally >12 m thick, primarily to the north. The flow field extends for 5.5 km along axis and covers a total area of 3.3 km^2; near its margins it grades into lobate and pillow lavas. It is bounded by the graben walls and clearly covers most of the faults on the graben floor to the north and south, yet the flow field itself is relatively untectonized. These features indicate that the Moai flow field is relatively recent, having been erupted inside the graben, and has not been affected significantly by subsequent tectonic activity.

[26] Three other features that are younger than most of the faulting and fissuring in the area were studied. Two small pillow mounds, <20 m high, cover areas of 0.11 and 0.15 km^2 just to the south of the Moai flow field. These

Table 2. Average Chemical Composition of Individual Southern EPR Lava Flows[a]

	Buddha		Animal Farm		Next Oldest		Aldo-Kihi		Moai		Rehu-Marka		Pillow Mounds		Lava Shield
	$n = 5$	σ	$n = 60$	σ	$n = 18$	σ	$n = 63$	σ	$n = 13$	σ	$n = 10$	σ	$n = 8$	σ	$n = 2$
SiO^2	50.8	0.13	50.8	0.17	50.5	0.19	50.3	0.28	50.2	0.24	50.0	0.16	49.6	0.45	50.01
TiO^2	1.65	0.01	1.65	0.02	1.44	0.03	1.54	0.07	1.35	0.05	2.00	0.01	1.28	0.05	1.34
Al_2O^3	14.4	0.05	14.5	0.09	15.1	0.14	14.8	0.22	15.4	0.15	14.1	0.10	15.8	0.18	15.7
FeO^*	10.7	0.05	10.6	0.08	9.65	0.11	9.96	0.26	9.63	0.18	11.2	0.18	9.44	0.19	9.75
MnO	0.19	0.01	0.20	0.01	0.18	0.01	0.18	0.01	0.18	0.01	0.21	0.01	0.18	0.01	0.17
MgO	7.28	0.03	7.29	0.05	7.91	0.08	7.87	0.21	8.12	0.13	6.79	0.03	8.44	0.06	8.35
CaO	11.7	0.04	11.7	0.07	12.3	0.13	12.2	0.15	12.5	0.10	11.3	0.06	12.4	0.12	12.4
Na_2O	2.98	0.01	2.96	0.04	2.78	0.05	2.53	0.09	2.60	0.08	2.94	0.11	2.61	0.05	2.64
K_2O	0.09	0.00	0.09	0.01	0.07	0.01	0.11	0.01	0.08	0.01	0.22	0.01	0.06	0.01	0.06
P_2O_5	0.14	0.00	0.14	0.00	0.12	0.01	0.13	0.01	0.11	0.01	0.21	0.01	0.10	0.01	0.10
Sum	99.9		99.9		100.1		99.6		100.3		99.0		99.9		100.6
HI	<1.0		1.20		1.41		2.00		1.62		1.26		1.87		

[a] All analyses by electron microprobe at University of Hawai'i; *n*, number of samples averaged; σ, one standard deviation from the mean. FeO^*, total Fe as FeO; HI, heterogeneity index [*Rubin et al.*, 2001].

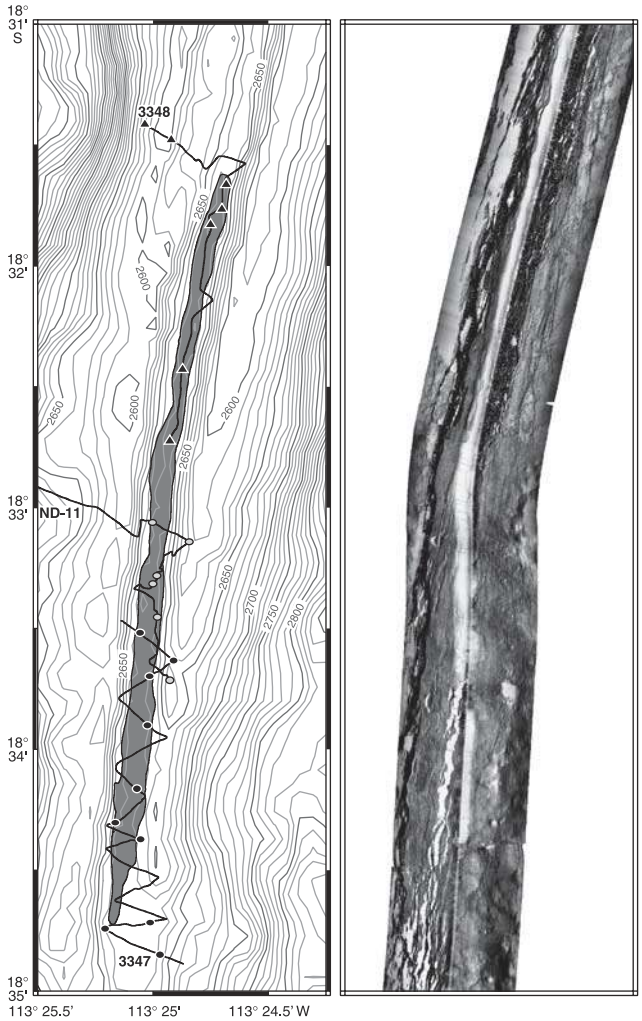

Figure 5. Map and side-scan sonar image of the South Hump region showing submersible dive tracks, sample locations, and the outline of relatively unfaulted lava in the South Hump region. South Hump lava is confined to the graben but is relatively unfaulted.

features were previously identified and described as pillow domes by *White et al.* [2000]. Another slightly elongate pillow complex with an overall morphology of a lava shield occurs near 18°21′S (Figure 9). This feature has an area of 1.1 km^2 and a summit elevation 30 m above the surrounding, heavily faulted seafloor. It is much larger than most of the lava domes described by *White et al.* [2000]. The summit region contains a crater ~50 m across and 5–10 m deep (Figure 9). All these pillow edifices consist of sparsely phyric, olivine + plagioclase-bearing lavas that show very limited evidence of posteruptive tectonic modification.

[27] The compositional variations for samples from this segment are shown in Figure 10. The great majority of samples from throughout the area, both within and outside of the axial graben, define a compositional field ranging from 7.0 to 7.8 wt % MgO (Figure 10). Some of the samples from this group come from heavily sedimented seafloor >2 km from the axis, whereas others come from delicate lava pillars from within the graben. This is an important result because it indicates that magmatic processes in this segment were relatively constant for a considerable length of time. Although individual lava flows can advance some distance from the axis, simple calculations predict that heavily sedimented seafloor 2 km from the axis in this area could be as much as 25,000 years old. Constant chemical composition over tens of thousands of years requires a balance between subvolcanic magmatic cooling and eruption on the one hand and recharge by new magma on the other. Furthermore, the recharge magma must have been relatively constant in composition during this time. Although *Auzende et al.* [1996] interpreted this composition to represent a single eruptive unit from a large lava lake, we now know that the samples defining this compositional range come from many different units erupted over a period that extends from hundreds to tens of thousands of years.

[28] All of the individual postgraben eruptive units described above have MgO contents that are much higher than the steady state composition for this segment (Figure 10), and all contain plagioclase phenocrysts. The Moai flow field shows a limited range in glass compositions with MgO from 7.9 to 8.3 wt % (13 analyses, Figure 10 and Table 2). The less well-sampled pillow mounds and lava shield have glass compositions with >8.35 wt % MgO. All these features have very similar chemical compositions, and it is possible that they collectively represent the products of a single eruptive sequence that produced localized, small-volume effusions along >20 km of ridge axis. Alternatively, they could reflect separate eruptive episodes. Available evidence indicates only that they all clearly postdate graben formation and most of the faults in the area and all are significantly less sedimented than other flows in the area. There are a few other samples in this area with >8.0 wt % MgO that we have not yet assigned to particular eruptive units. There also are some samples that have <7 wt % MgO. These mainly come from relatively old lava pillars and other features representative of ancient lava lakes in the axial region. It is notable that compositional data for the Moai lava lie on the high-MgO extension of the large population of samples having <8 wt % MgO. However, samples from the small pillow mounds and lava shield define a parallel trend with slightly higher TiO_2 and FeO^* and lower CaO (Figure 10).

[29] Chemical and geological data obtained for this region provide constraints on the long-term magmatic and tectonic evolution of this ridge segment. For at least a few tens of thousands of years, this segment erupted lavas with relatively uniform compositions, possibly with rare and and/or local excursions to more primitive or more evolved compositions. Moderately high and broad flanks of the segment suggest that it was in a state of high magmatic flux during at least the early part of this period. Similar compositions have been found within the graben, including some delicate lava pillars that are unlikely to have survived major collapse. Hence as tectonism became more important than volcanic construction in the region, similar compositions continued to be erupted. More recently, however, this segment has seen a change to higher magnesian magmas, erupted in relatively small volume flow fields that clearly postdate much of the

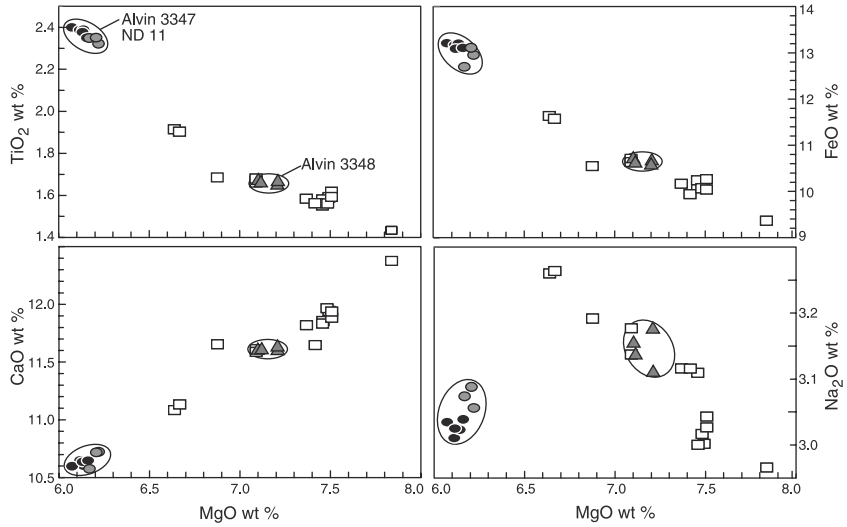

Figure 6. Chemical compositions of lavas from the South Hump region. South Hump ferrobasalts from NAUDUR dive 11 and *Alvin* dive 3347 are shown as ovals; *Alvin* dive 3348 samples from the relatively unfaulted part of the graben floor are shown as triangles. ND-11 ferrobasalts are slightly more magnesium that those collected farther to the south during *Alvin* dive 3347. It is notable that the South Hump ferrobasalts have much too low Na to be derived from the higher magnesian South Hump magmas by fractionation. See text for discussion.

faulting in the graben floor. The high-MgO contents reflect recent recharge of primitive magma that has been less affected by cooling prior to eruption. In terms of volcanic-tectonic cycles, if such a model pertains to this segment, then the region may be near the beginning of a new cycle of increasing magmatism. This period comes after an early period of robust magmatism, followed by a period of increased tectonism and graben formation.

2.4. Aldo-Kihi Lava

[30] Results of the NAUDUR program indicated that very recent volcanism occurred in the region near 17°26′S.

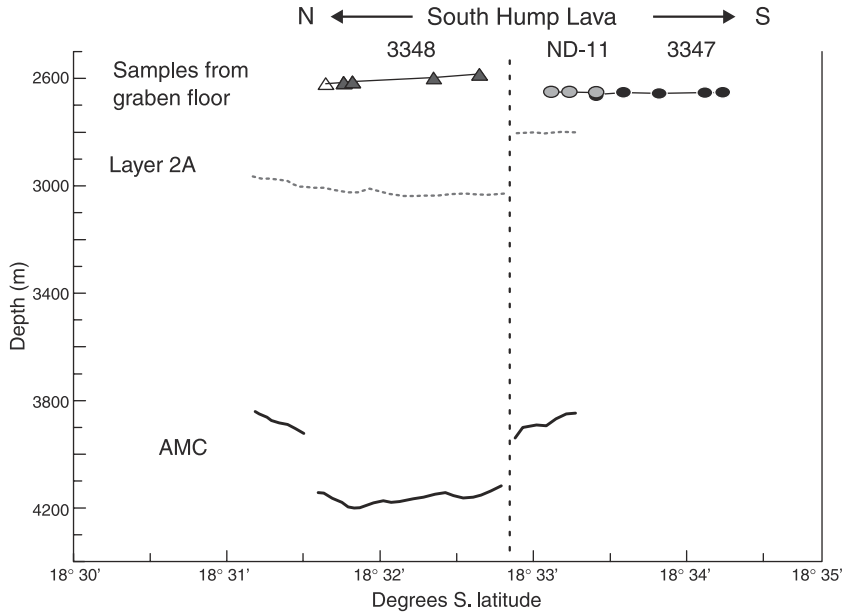

Figure 7. Along-axis variations in graben floor depth and sample locations (top symbols, same as in Figure 6), the thickness of layer 2A (subhorizontal dashed line) and the depth to the top of the axial magma chamber (AMC) seismic reflection (heavy shaded line); 2A thickness and depth to AMC from *Hooft et al.* [1997] in the South Hump region. The vertical dashed line marks a break in AMC depth, layer 2A thickness, and chemical composition of graben floor samples (see Figure 6); in contrast, the side-scan sonar data suggest that the graben throughout this region is floored by relatively unfaulted lava with generally similar reflectivity.

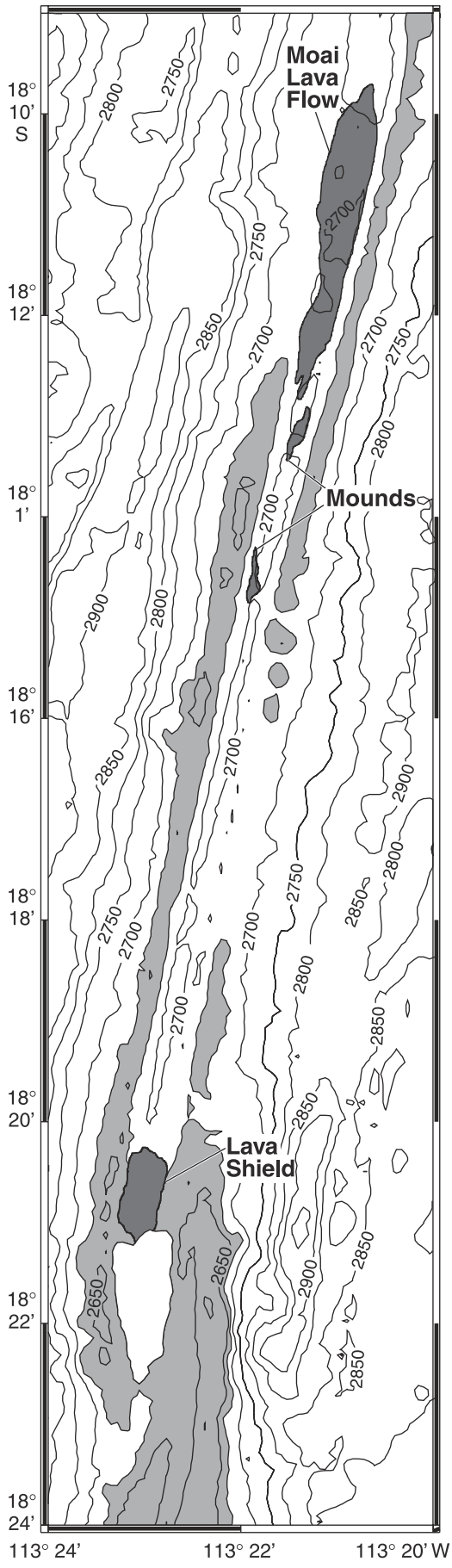

The nearly complete lack of covering sediment and association with a spike in the subaxial magma chamber reflector [*Mutter et al.*, 1995] suggests that at least some of this activity probably occurred in the early 1990s. This discovery, along with the presence of numerous areas of hydrothermal activity, led many other investigators to visit this area in subsequent years. *Embley et al.* [1998] mapped the boundaries of a young lobate lava flow field between 17°32.5′S and 17°34′S. They designated this flow L0 and proposed that it was part of the same eruptive sequence identified by *Auzende et al.* [1994, 1996] near Lake Aldo and the Kihi hydrothermal field farther north. Using previously collected DSL 120-kHz sonar and ARGO II data for this area [*Haymon et al.*, 1997; *White et al.*, 2000], along with nine new *Alvin* dives and nighttime sampling stations, we mapped the boundaries of this young lava flow field (Aldo-Kihi) covering the axis between 17°24′S and 17°34′S (Figure 11). Contacts between the Aldo-Kihi field and surrounding geologic units were identified on the basis of differing sediment cover and lava flow morphology observed from *Alvin*. The Aldo-Kihi flow field was erupted along 18.5 km of ridge axis and covers an area of 14 km^2. Its maximum width is 2.2 km at 17°27′S; in this area the flows show evidence for moderately high effusion rates. The most common lava morphology in this area is lobate, although a number of lava channels floored with lineated and jumbled sheet flows were observed to trend both along and across the axis. Between 17°26′S and 17°28′S, there are seven en echelon summit collapse troughs 100–500 m long, up to 50 m wide (Figure 11) and up to 12 m deep. Two of these, Lake Aldo and the adjacent one to the south encompassing the Kihi hydrothermal field, give the flow field its name. Between 17°28′S and 17°28.5′S, branching, partially collapsed lava tube systems up to 220 m long and 30 m wide, first noted on 120-kHz side-scan sonar images [*White et al.*, 2000], were observed to trend down the west side of the axis. Numerous collapse pits in lobate lava show that these flows are locally >12 m thick. The concentration of large summit collapse troughs and collapsed lava tubes suggests that eruptive activity in the Aldo-Kihi flow was concentrated near 17°27′S. Between 17°29′S and 17°34′S, collapse features are much less prevalent, the flow field is narrower (150–500 m), and lava morphology is dominantly pillow and lobate, suggesting that the total extruded volume and effusion rate were significantly lower in the southern part of the field [*Embley et al.*, 1998].

[31] Fifty microprobe glass analyses of Aldo-Kihi lava show that MgO contents range from 7.7 to 8.4 wt %; all the samples with >8.0 wt % MgO occur south of 17°30′S (Figure 12). Two hypotheses could explain the along-axis variation in lava composition of the Aldo-Kihi flow field. One is that the region of highest MgO (near 17°31′S)

Figure 8. (opposite) Map of the rifted segment between 18°10′S and 18°23′S showing the outcrop areas of the Moai lava flow field, small pillow mounds, and lava shield. Depths <2670 m are shaded to emphasize the presence of the flanking ridges outside of the axial graben. Contour interval is 50 m. Lava features discussed in the text are all confined to the graben.

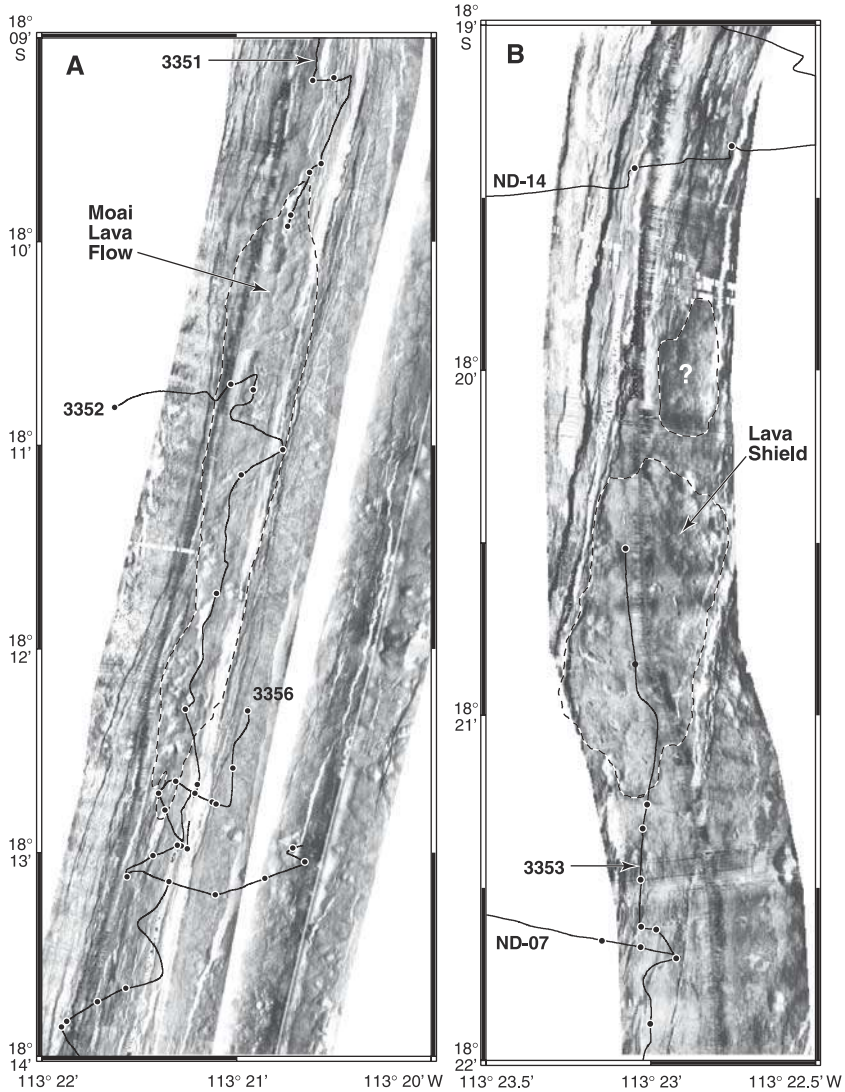

Figure 9. DSL 120 kHz side-scan sonar images of features shown in Figure 8. Submersible dive tracks and samples locations are shown. (a) Region between 18°10′S and 18°15′S, showing Moai lava flow field and small pillow mounds. The western side-scan swath was collected during the Sojourn expedition [*Haymon et al.*, 1997; *White et al.*, 2000] and the eastern swath during the STOWA cruise. Note contrast between the heavily faulted terrain outside of the outlined lava features and the apparently more recent flows. The presumed eruptive center of the Moai flow field is near 18°10.5′S, where lava channels are prominent and the flow morphology is a jumbled sheet flow. To the north and south the field grades into lobate and pillow lavas. (b) Lava shield with small summit crater near 18°21′S. Side-scan images are from same swaths shown in Figure 9a.

marks the eruptive center and that the decrease in both directions represents syneruptive fractionation [*Shibata et al.*, 1999]. However, it is clear that the greatest volume of lava with the highest effusion rates was erupted farther north, between 17°26′S and 17°28′S. If this region of axial collapse troughs, abundant lava tubes, and open lava channels is the eruptive center, then the along-axis chemical variation may indicate that the eruptive dike(s) tapped a subvolcanic magma reservoir that was chemically variable along axis [*Bergmanis et al.*, 1999]. Because we interpret the geological evidence to suggest that the eruptive center was well north of 17°29′S, we presently favor this latter explanation. On the basis of structural criteria, *White et al.* [2000] identified a volcanic segment boundary separating the regions north and south of 17°30′S, i.e., within the Aldo-Kihi flow field. They suggest that these segments are moderately long-lived features, persisting for 0^3–10^5 years. Whether or not the chemical contrast and possible gradation in along-axis composition of the subaxial magma reservoir also are long-lived is unknown.

[32] There is evidence for multiple eruptive events within the Aldo-Kihi lava field (Figure 13). For example, a thin flow of unsedimented lava was seen to cascade into collapse pits on dive 3360. Although many of the collapse structures in the axial region of this field may be syneruptive, the cascading lava appears to be slightly less

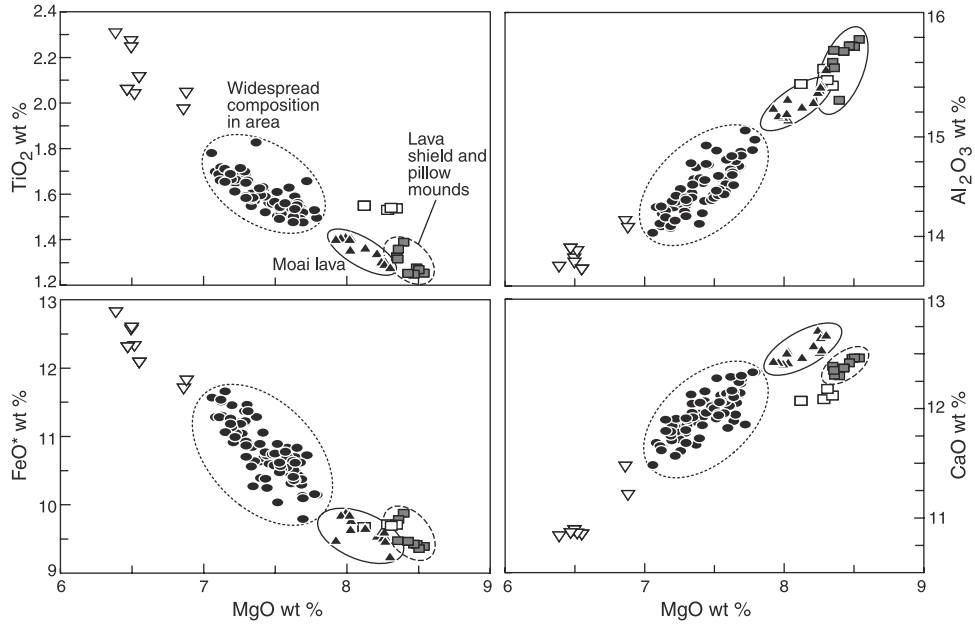

Figure 10. Chemical variations of samples from the region shown in Figure 8. The large field with 7–8 wt % MgO comprises samples from throughout the area, including heavily sedimented samples from outside the graben >2 km away from the present axis. None of these samples comes from features interpreted to be among the youngest, i.e., obviously younger than much of the faulting in the area. Samples from the Moai flow field, pillow mounds, and lava shield all have >7.8 wt % MgO. Other samples from the region are shown with open symbols. Open squares are other high magnesium samples not yet assigned to particular eruptive units. See text for discussion.

sedimented than the surrounding lava, and therefore somewhat younger. On dive 3365 near 17°26′S, two lava flows occur in a region where there has been extensive hydrothermal activity. Several millimeters of hydrothermal sediment covers older lobate lavas, with sediment thickness increasing toward an extinct hydrothermal chimney up to 10 m high. A small flow of very glassy pillow lava that is devoid of hydrothermal sediment overlies sedimented lobate lava (Figure 13c) close to the extinct chimney. Both of the lava flows in this area are within the boundary of the Aldo-Kihi lava flow field shown on Figure 11. In this case the younger, posthydrothermal lava appears to have been erupted after the main part of the Aldo-Kihi lava and most of the hydrothermal activity in the area. This same flow and its contact with more sedimented lava was identified during NAUDUR dive 3, indicating that it was emplaced prior to December 1993. Thus it is clear that some flows that we have combined into the Aldo-Kihi flow field are younger than others and that the boundaries of Aldo-Kihi can be considered to comprise multiple individual lava flows, apparently from separate eruptive events. The mappable age contrast between Aldo-Kihi and older lavas in the region suggests that the Aldo-Kihi flow field constitutes a single eruptive episode.

[33] In some areas the Aldo-Kihi lavas can be easily distinguished from older flows on the basis of composition alone, but in others, there is essentially no compositional change across contacts identified on the basis of contrasting sediment cover and flow morphology during submersible operations. This suggests that this length of ridge has erupted compositionally similar lavas in separate volcanic episodes. Thus, although chemical mapping [e.g., *Reynolds et al.*, 1992; *Perfit et al.*, 1994; *Batiza et al.*, 1996] can provide valuable insight into interesting variations in ridge magmatic processes, in at least some areas it is an unreliable way to map the products of single volcanic episodes.

[34] In addition to the Aldo-Kihi lava we collected samples and observations on two other lava units in the area (Figure 11). The Rehu-Marka lava is a distinctive Fe- and Ti-rich lava that hosts several important hydrothermal sites [e.g., *Fouquet et al.*, 1994; *Urabe et al.*, 1995]. Our study and NAUDUR observations show that this unit was erupted in at least two phases, an earlier, highly jumbled sheet flow, and a later, lobate lava that extends only a few hundred meters from the present axis (Figure 11). Lavas along the axis north of 17°24.5′S were sampled during the NAUDUR expedition; the composition of these lavas overlaps that of the younger Aldo-Kihi lavas but are more sedimented. Similar compositions also occur immediately to the east side of the Aldo-Kihi flow field south to 17°28′S. Along this contact, there is a distinctive increase in sediment cover to the east. Whether or not the various observed localities of uniform chemistry older than Aldo-Kihi all represent part of a single eruptive episode is unknown.

3. Discussion

3.1. Volcanic Eruptions at Superfast Spreading Midocean Ridges

[35] Some characteristics of the lava units discussed above are given in Table 1. Eruptive fissures vary from

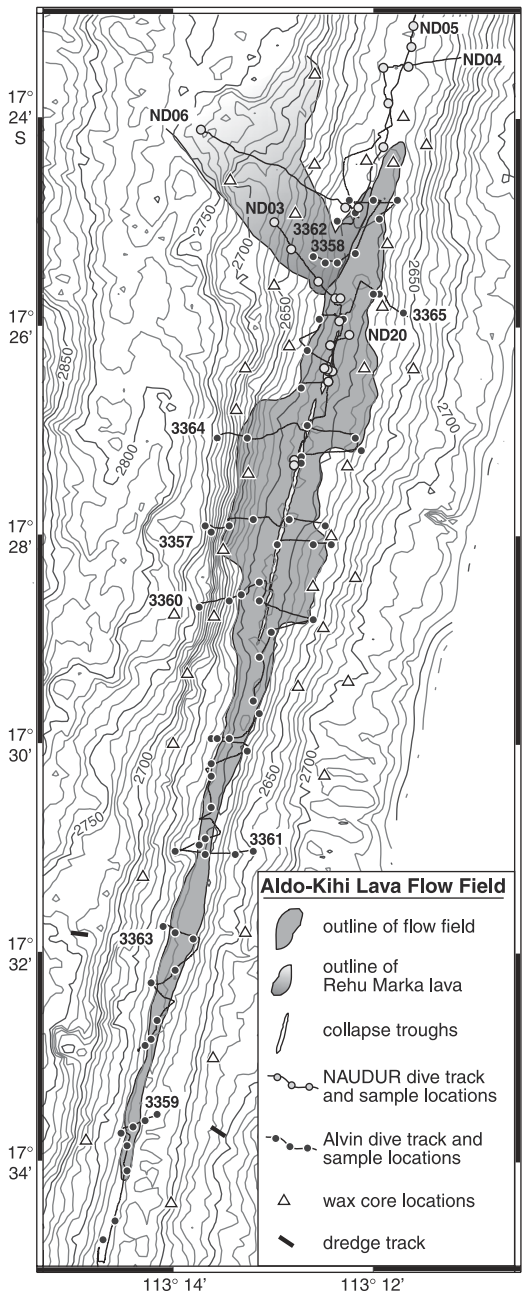

Figure 11. Map of the Aldo-Kihi lava flow field; a partial outline of the Rehu-Marka flow field also is shown. The boundaries of the Aldo-Kihi flow field (dashed where less certain) primarily reflect the locations of observed age contrasts from submersible, although chemical variations were used in places to distinguish the Aldo-Kihi lava from Rehu-Marka. Note the strong decrease in flow field width south of 17°29′S. Well-developed axial troughs, lava channels, and collapsed lava tubes are mainly restricted to the region between 17°26′S and 17°28′S.

<1 to >18 km along axis. Although some intragraben flow fields are confined by structural controls, unconfined lava erupted from axial highs does not exceed distances greater than ~2.5 km from the axis. This distance is much less than predicted from cooling considerations [e.g., *Head et al.*, 1996; *Gregg and Fornari*, 1998], suggesting that the off-axis lengths of lava flows in this area are limited by supply at the vent, rather than by cooling during flow. Sheet flows with axis-parallel flow directions are common in the summit troughs, providing evidence for significant along-axis movement of lava within the vent regions of some units.

[36] Thicknesses of individual units can be estimated from the depths of collapse pits and troughs within them, by relationships to partially buried fault scarps, and from inferences based on edifice morphology. Although such estimates are subject to various uncertainties and generally only provide minimum thicknesses, we consider our estimates to be accurate to within a factor of 2. We estimate average thickness of the flow fields to range from ~3 m (Buddha Flow) to 12 m (Animal Farm). Lava flow field volumes in this area, as in most volcanic terranes, are overwhelmingly dominated by their surface areas. Of the

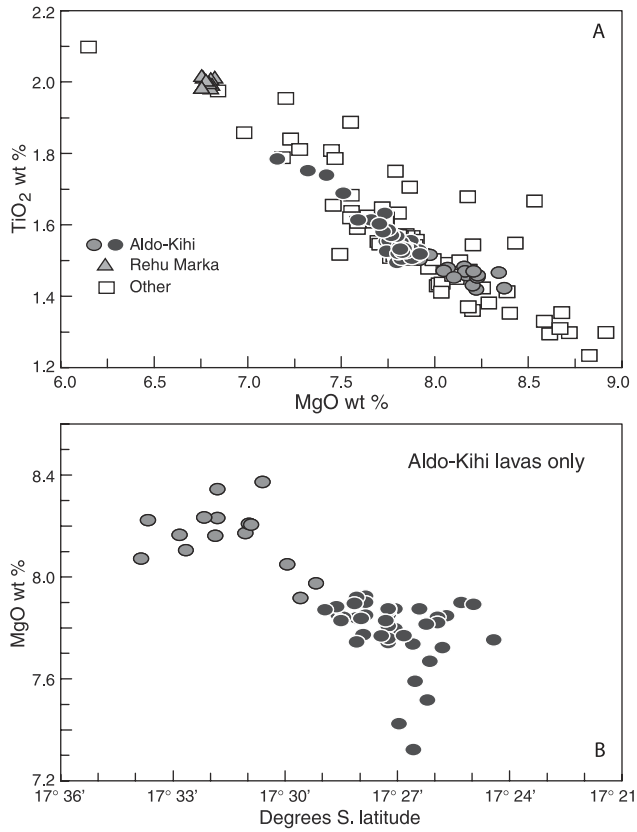

Figure 12. Chemical variations from the region shown in Figure 11. Aldo-Kihi samples from north of 17°29′S where the flow field is wide are shown with dark shading; samples from the narrow part of the flow field south of 17°29′S are shown by lighter shading. (a) The linear variation of Aldo-Kihi lava samples over the range of MgO from 7.7 to 8.4 wt %, consistent with evolution by variable fractionation within a common magma reservoir. (b) Along-axis variation in composition of Aldo-Kihi lava samples, showing the along-axis variation in MgO content. All the samples with >8 wt % MgO are from south of 17°30′S. See text for discussion.

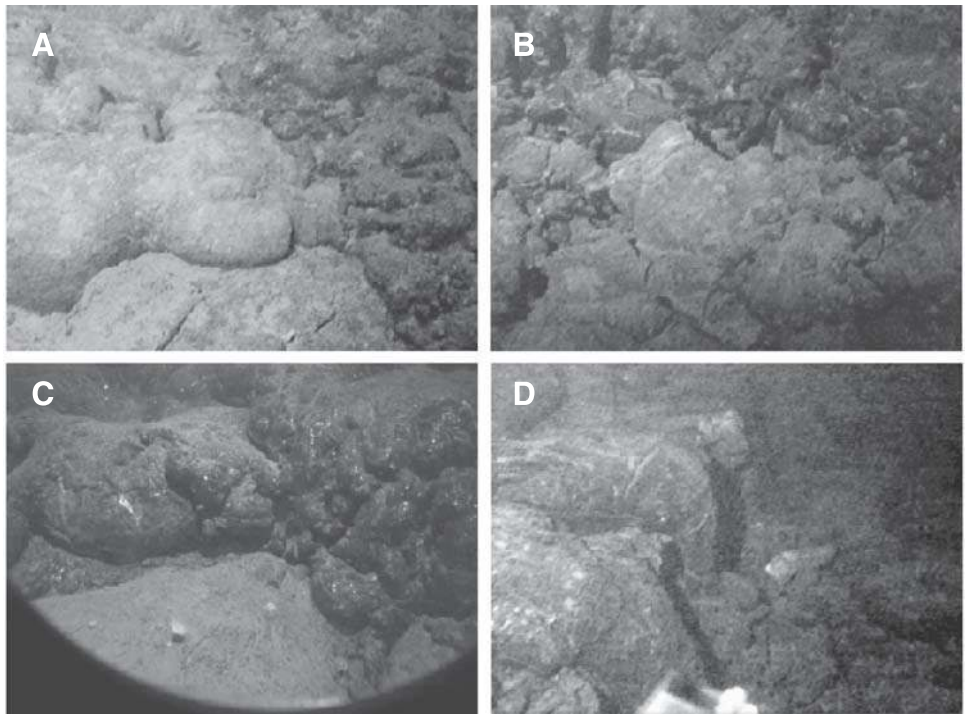

Figure 13. Photos showing a range of contact relations of the Aldo-Kihi lava flow field. Figures 13a and 13b show contacts along the western boundary of the Aldo-Kihi lava, where relatively unsedimented, slightly pillowed Aldo-Kihi lava overlies older lobate lavas with similar major element composition. (a) *Alvin* dive 3357, 17°27.83′S, 113°13.43′W; Aldo-Kihi lava on right side. (b) *Alvin* dive 3364, 17°27.03′S, 113°13.32′W; Aldo-Kihi lava on top. Figures 13c and 13d show internal contacts within the Aldo Kihi lava flow field. (c) Internal contact showing the latest phase of pillow lava overlying slightly earlier Aldo-Kihi lobate lava flow, now partially covered by hydrothermal sediment and an anemone; *Alvin* dive 3365, 17° 25.91′S, 113°12.31′W. (d) Latest Aldo-Kihi lava spilling into recent collapse pit within slightly older Aldo-Kihi lava; *Alvin* dive 3360, 17° 29.13′S, 113°13.13′W. Horizontal dimensions of Figures 13a, 13b, and 13d are ~5 m; horizontal dimension of Figure 13c, taken through the *Alvin* pilot's view port, is ~3 m. See color version of this figure at back of this issue.

seven completely mapped flow fields listed in Table 1, estimated erupted volumes vary by 3 orders of magnitude, and hence uncertainties in thickness represent a relatively minor component of the variation. The largest unit (Animal Farm) has a volume of $\sim 220 \times 10^6$ m^3. The average volume of the seven completely mapped flow fields is 51×10^6 m^3, but most of the units have small volumes, and the median value is $\sim 9 \times 10^6$ m^3. Assuming that erupted volumes of $10-50 \times 10^6$ m^3 are typical for the southern East Pacific Rise and that the upper 500 m of the oceanic crust is extrusive, one could expect an eruptive episode approximately every 3–14 years for each 50-km-long segment. This frequency is in general agreement with estimates of *Macdonald* [1998].

[37] The widespread presence of sheet and lobate lava indicates that eruptions with relatively high effusion rates (>100 m^3/s for lava viscosities of 10^2 Pa s) are common in this area [e.g., *Gregg and Fink*, 1995]. The combination of low erupted volumes with high effusion rates suggests that eruptions in this area are likely to be both frequent and short-lived. Eruption durations calculated for the lava volumes of Table 1 are of the order of hours to weeks, similar in duration to seismic events detected on mid-ocean ridges [*Einarsson and Brandsdottir*, 1980; *Dziak et al.*, 1995; see also http://www.pmel.noaa.gov/vents/acoustics/seismicity/seismicity.html]. Although sheet and lobate lava are the most common flow morphologies observed in our study, pillows occur at the distal ends of several fissures and on the lateral edges of most flow fields; pillows make up the entire eruptive sequence in some small units within the two rifted segments that we studied. The transition from sheet and lobate lavas to pillow lava at the edges of individual eruptive units is similar to those occurring along several third-order structural segments in this area [*White et al.*, 2000]. Although we have observed along-strike transitions occurring within single eruptive episodes, the well-documented propensity for pillow eruptions at segment ends [*White et al.*, 2000] suggests that the along-axis variations in volcanic style may characterize multiple eruptions over significant periods of time.

3.2. Spreading Rate Dependence of Volcanic Eruptions at Mid-ocean Ridges

[38] Few eruptive sequences on submarine mid-ocean ridges have been studied. *Embley and Chadwick* [1994, 1994], *Smith et al.* [1994], *Chadwick et al.* [1995, 1998], *Smith* [1999], *Rubin et al.* [1998], and *Embley et al.* [2000] studied a number of flow fields from the inter-

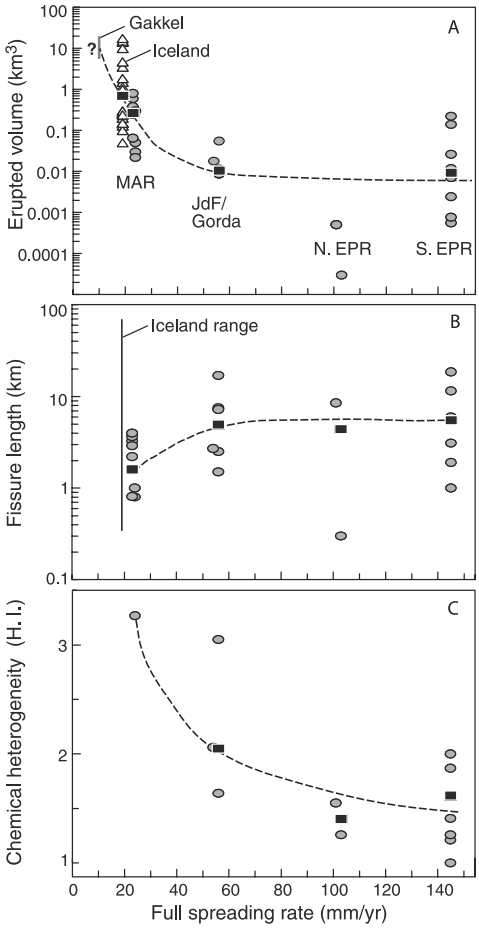

Figure 14. Volcanic variations versus spreading rate. Despite the general dearth of data for submarine mid-ocean ridge eruptions, the apparent various trends are consistent with expected variations in magma chamber processes and thermal structure of mid-ocean ridges. See text for discussion. Solid squares are median values for the parameters shown. (a) Volumes produced during single eruptive episodes. Southern EPR (S. EPR) volumes are those reported in this paper. Those from the Juan de Fuca and Gorda Ridges (JdF/Gorda) are from *Perfit and Chadwick* [1998] and *Rubin et al.* [2001]; those from the northern EPR (N. EPR) are from *Gregg et al.* [1996] and *Rubin et al.* [2001]. Mid-Atlantic Ridge (MAR) volumes are estimated from edifice morphology [from *Perfit and Chadwick*, 1998]. Iceland volumes represent a compilation from various sources, mainly *Saemundsson* [1991, 1992], *Gundmundsson* [1996], and *Sinton* [1997a, also unpublished data]. The flow field area from the western construct along the Gakkel Ridge is from *Edwards et al.* [2001]. The 6.6–11 km^3 volume shown assumes an average thickness of 30–50 m for this flow field. (b) Eruptive fissure lengths for single eruptions versus spreading rate for submarine mid-ocean ridge eruptions. Short fissure lengths appear to be favored at slow spreading ridges. Known fissure lengths in Iceland range from a few hundred meters to 70 km. References are same as those listed for Figure 14a. (c) Heterogeneity Index [*Rubin et al.*, 2001] versus spreading rate. Values for fast and intermediate spreading ridges and for Serocki Volcano are from *Rubin et al.* [2001]. Compared to eruptive sequences at lower spreading rates, those from the S. EPR are relatively homogeneous (low HI).

mediate spreading Juan de Fuca and Gorda Ridges and provided important details on eruptive areas, volumes, and internal characteristics. Two small flows on the fast spreading northern East Pacific Rise have been studied [*Haymon et al.*, 1993; *Rubin et al.*, 1994; *Batiza et al.*, 1995; *Gregg et al.*, 1996]. The lava flow fields described here extend those observations to superfast spreading and nearly double the catalogue of individual eruptive sequences on submarine mid-ocean ridges. Since the early investigations in the FAMOUS and AMAR regions [e.g., *Ballard and van Andel*, 1977; *Bryan and Moore*, 1977; *Hekinian et al.*, 1976; *Luyendyck and Macdonald*, 1977; *Crane and Ballard*, 1981; *Stakes et al.*, 1984], there has been little detailed study of volcanic features on slow spreading ridges that combines mapping and flow field-scale chemical study. Estimates of eruption volumes at slow spreading ridges have been derived from the morphology of edifices that are presumed to be monogenetic volcanic features [e.g., *Crane and Ballard*, 1981; *Smith and Cann*, 1990; *Perfit and Chadwick*, 1998]. *Ballard and van Andel* [1977] and *Crane and Ballard* [1981] provided geological observations supporting the interpretation that many of these edifices are probably single volcanic constructs. In contrast, *Edwards et al.* [2001] identified a lava flow field covering ~220 km^2 along the very slow spreading Gakkel Ridge. They concluded that this field was probably formed during at least two eruptions, but the contrasting sonar reflectivity of this field compared to that of the surrounding seafloor suggests that these eruptions may have been close in time. *Edwards et al.* [2001] concluded that volcanic activity along this ridge may be episodic.

[39] Results from our study of the southern East Pacific Rise are combined with data from other spreading ridges on Figure 14. This is essentially the entire present data set for submarine mid-ocean ridge eruptions. It is obvious that many more data are required before rigorous comparisons can be made. For example, one might expect that almost any area will experience a wide range of eruptive volumes over time, with very large eruptions being relatively rare. The lengths of eruptive fissures also might be expected to be quite variable as well as the chemical heterogeneity of single lava units. Ideal comparisons involve medians from a size-frequency analysis of statistically significant data sets, but the existing data set is probably too meager to be statistically significant. As such, whether or not the apparent relationship that eruptions along the Mid-Atlantic Ridge tend to be larger than those at faster spreading ridges or that eruptions in Iceland are typical of slow spreading ridges irrespective of magma supply will hold up to further data remains to be seen. The extension of the apparent increase in erupted volume with decreasing spreading rate to the very slow spreading Gakkel Ridge is highly speculative because the number of eruptions involved in the identified flow fields is unknown and the total volume also is unconstrained by existing data (see Figure 14 caption). However, there are a number of reasons to suspect that there should be a spreading rate dependence to eruption volume; that is, that the general relationship apparent in Figure 14a is valid, as discussed below.

[40] One important characteristic of ridges spreading at full rates greater than ~60–80 mm/yr is the presence of

essentially steady state, eruptible magma lying beneath a thin, weak lid [e.g., *Sinton and Detrick*, 1992]. It is likely that such reservoirs have internal, excess magma pressures that are close to those required to initiate dike propagation. Therefore eruptions should be easily triggered, for example, by incremental seafloor spreading events or small increases in magma pressure, arising either from recharge or magmatic differentiation. In contrast, magma reservoirs almost certainly are intermittent at slow spreading ridges and commonly form beneath thicker and stronger lids [*Buck et al.*, 1997]. Because critical excess magma driving pressure is a function of both depth and the strength of the overlying crust [e.g., *Rubin*, 1993], higher excess pressures may be required to initiate eruptions in such settings. The relationship between excess magma driving pressure and erupted volume is not direct, however, although *Buck et al.* [1997] have shown a relationship between magma lens depth and the thickness of layer 2A, which many authors take to represent the extrusive layer. Thus significant magma buildup prior to eruption might be required to initiate dike propagation beneath thick lids. However, once initiated, large volumes of magma are erupted. Furthermore, because overburden pressures are greater for deep magma reservoirs, it is likely that a greater proportion of the available magma will be erupted from deep magma reservoirs than from shallow ones.

[41] Another possible reason why fast spreading ridges might typically experience lower volume eruptions concerns the relative partitioning of magma involved in an event between the effusive (lava) and intrusive (dike) components. A number of studies suggest that point source pillow mounds are a common product of eruptions along the Mid-Atlantic Ridge [e.g., *Ballard and van Andel*, 1977; *Smith and Cann*, 1990, 1992; *Lawson et al.*, 1996], although more elongate features and sheet flows also locally occur. In contrast, many eruptions along the southern East Pacific Rise appear to be fed by relatively long fissures (Figure 14b), although constructional pillow edifices also occur, especially near segment ends [*White et al.*, 2000]. The Aldo-Kihi fissure system described in this paper is the longest yet documented from any submarine mid-ocean ridge, although some eruptive features along the Juan de Fuca Ridge are almost as long [e.g., *Embley et al.*, 2000]. Thus evidence suggests that lateral magma transport may be favored at intermediate and fast spreading ridges, where a strong tensional stress may occur over significantly longer ridge lengths than for slower spreading ridges. Although lava flow field mapping can determine the amount of lava erupted onto the seafloor, the amount of magma involved in an event or episode that is not erupted remains unknown for most cases.

[42] During the 1975–1984 Krafla eruptions in northeast Iceland, $\sim 200 \times 10^6$ m^3 of lava was erupted during a series of events for which estimates based on inflation/deflation measurements suggest $\sim$3 times that amount was expelled from a reservoir lying beneath Krafla caldera [*Tryggvason*, 1984, 1986; *Bjornsson*, 1985; *Harris et al.*, 2000]. Because shallow magma chambers beneath the East Pacific Rise probably reside just below their levels of neutral buoyancy [*Hooft and Detrick*, 1993], the probability of overshooting this level during an eruption is much less than for eruptions rising from deeper magma chambers. Hence it is more likely that dikes will become entrained along the level of neutral buoyancy at fast spreading ridges and that significant proportions of the magma involved in an event might never reach the surface. In this scenario the total amount of magma involved in an event might not be significantly different in ridges spreading at different rates, only the proportion of this magma that eventually reaches the surface. Lower extrusive/intrusive volume ratios at faster spreading ridges would primarily be accommodated in longer dikes for individual events (e.g., Figure 14b) beneath the East Pacific Rise but also is consistent with a thinner seismic layer 2A thickness [*Buck et al.*, 1997].

3.3. Chemical Heterogeneity

[43] The chemical heterogeneity of individual eruptive episodes has important implications for the nature of the underlying magma reservoirs as well as for processes occurring during eruptions. Among the flow fields investigated in this study, most show only a limited range of compositional variation although one unit is distinctly bimodal (South Hump) and one shows an along-axis pattern of variability (Aldo-Kihi). The largest flow field (Animal Farm) is extremely uniform in composition. Thus it is apparent that there is a range of heterogeneities that can characterize lava eruptions at superfast spreading ridges and that some of this variability is unexpected (South Hump). *Rhodes* [1983] and *Rubin et al.* [1998, 2001] quantified the chemical heterogeneity of lava flows using a heterogeneity index (originally homogeneity index [*Rhodes*, 1983]). This index is defined as $\Sigma(S_i/P_i)/n$, where S_i/P_i represent the 2σ deviation from the mean of the data divided by the analytical precision for each element i and n is the number of elements used in the determination. Lavas with an index of 1.0 are uniform within analytical precision for all elements analyzed. Heterogeneity Indices (HI) for southern EPR lavas vary from <1.0 to 2.0 (Table 2). Although *Rubin et al.* [1998] found a general correlation of HI with erupted volume [see also *Sinton*, 1997a], southern EPR lavas belie this correlation because the Animal Farm lava is the most voluminous but also is the most homogeneous.

[44] There are various ways to interpret chemical variability, or lack thereof, over the axial length of an eruption. If dikes primarily rise vertically, then the variability along axis can be a monitor of the along-axis variation in the subaxial reservoir. However, there is abundant evidence that dikes can propagate for tens of kilometers in the crust during mid-ocean ridge rifting events [*Einarsson and Brandsdottir*, 1980; *Dziak et al.*, 1995]. Although there still are far too few data to be representative of the broad spectrum of mid-ocean ridges, it is notable that the eruptions from the superfast spreading southern East Pacific Rise generally show less variability than those from intermediate spreading centers [*Perfit and Chadwick*, 1998; *Rubin et al.*, 2001], which include some of the best defined eruptive units prior to this study. The fact that few of these earlier defined flow fields have been sampled as extensively as in our study further emphasizes the generally limited chemical heterogeneity along the southern East Pacific Rise. Thus existing data suggest an inverse relationship between chemical heterogeneity of

eruptive units and spreading rate [*Rubin et al.*, 2001]. This relationship is consistent with the presence of magma reservoirs at high spreading rates that are relatively well mixed over significant volumes.

[45] One important conclusion from our study concerns the chemical uniqueness of individual flows and flow fields. We have shown that different flows spanning an age range up to tens of thousands of years can be generally similar in chemical composition. This result also is consistent with the presence of relatively large, well-mixed magma reservoirs and further indicates that, at least in some cases, these reservoirs can be long-lived. It is clear that the rate of eruption greatly exceeds the timescales over which some of these reservoirs are changing composition, either from significant differentiation or by variable melting processes in the underlying mantle. Although chemical mapping using closely spaced samples in the absence of geological observations clearly is an inadequate way to map individual volcanic eruptions at superfast spreading, this approach is one way to assess the spatial and temporal variability of magmatic processes along individual ridge segments.

3.4. Episodicity of Mid-ocean Ridge Volcanic Activity

[46] One of the key questions addressed in this paper is "What constitutes an eruption episode?" As discussed in section 1, there is a hierarchy in the Krafla system involving individual lava flows, isolated eruptive events, rifting episodes, and major rifting periods. Real-time observations during the Krafla episode allowed individual lava flows and isolated eruptive events to be identified. However, the finest resolution that would be likely to be distinguished from later mapping efforts is the products from individual episodes, which are separated at Krafla by at least several hundreds of years. *Embley et al.* [2000] described the products of three separate eruptions occurring over ~12 years along the CoAxial segment of the Juan de Fuca Ridge, although in this case the products are isolated lava fields that have been identified by later detailed surveying and sampling of the ridge axis. Along the southern East Pacific Rise, the South Hump lavas appear to have been emplaced after a period of major tectonic activity and, in this regard, can be ascribed to a new eruptive episode in that area. This interpretation is reasonable irrespective of whether the South Hump lavas represent a single, bimodal eruption or two separate eruptions, close in time. Similarly, the Moai flow field, lava shield, and pillow mounds occurring between 18°08′S and 18°22′S also appear to represent recent activity that postdates major tectonic events. However, exactly how many individual eruptions are responsible for these features and the time breaks between them is unknown. Thus they could represent individual events within an episode or separate episodes within a major rifting and magmatic period.

[47] In those areas where the axis shows an inflated morphology the distinction among the products of separate events or episodes is even more difficult to discern. For example, we have evidence that the Aldo-Kihi flow field is composed of more than one lava flow, apparently produced by separate eruptions close in time. Although we have also been able to identify at least three separate lava flow units in the Animal Farm area, the time breaks between each of these events are unknown. Chemical variations suggest a fundamental change in the composition of the magma between the next oldest flow field and Animal Farm, although the time break separating these two units was short enough to prevent significant sedimentation of the next oldest flows prior to onset of the Animal Farm eruptions. Although the Buddha Flow is compositionally identical to Animal Farm, it is obviously less sedimented; stratigraphic relations at the contact indicate that it definitely is younger. Because Animal Farm appears to be less than 100 years old based on our geological observations and its magnetic paleointensity [*Carlut and Kent*, 2000], the time interval between emplacement of Animal Farm and the Buddha Flow can be no more than a few years to decades.

[48] A consequence of the apparent decrease in median erupted volume with increasing spreading rate (Figure 14a) is that the frequency of eruption increases and the period between eruptions decreases. For a given spreading rate, crude calculations of eruption period (the time between eruptive episodes) can be made from the median erupted volumes and assumptions about the thickness of the extrusive layer. Assuming that this latter parameter increases from 500 m at the southern EPR to 700 m at the Juan de Fuca Ridge to 1000 m along the Mid-Atlantic Ridge, the calculated eruption periods increase from 6.5 years to 13.4 years to 590 years, respectively. Although there are significant uncertainties in some of the values used to calculate eruption periods, it is unlikely that those uncertainties will offset the apparent difference of 2 orders of magnitude between the Mid-Atlantic Ridge and southern East Pacific Rise. As eruption period decreases, the distinction between eruptive events, rifting episodes, and major rifting periods obviously becomes blurred. Thus it is our conclusion that one of the major problems in carrying out our investigations at superfast spreading, namely, the difficulty in identifying discrete eruptive episodes along some locations of the ridge, is one of our most important results. At the highest spreading rate time breaks between major rifting periods, eruptive episodes and eruptive events begin to converge at values of no more than a few years; that is, fast spreading ridges are less episodic volcanically than are slower spreading ridges. Although this creates some problems in classifying erupted products into discrete eruptive episodes, the advantage of frequent eruptions is that it provides a finer temporal resolution of the underlying magmatic processes. This resolution can be fully exploited when chemical study of the erupted lavas is combined with geologic mapping and constraints on lava ages.

4. Conclusions

[49] The most important conclusions from this study are as follows:

1. Seven newly mapped lava flow fields along the southern EPR cover areas of <0.2 to >18 km^2, with estimated volumes of <1 to ~220 × 10^6 m^3. The lengths of axial fissures activated during the events that produced these lavas range from ~1 to >18 km. Two other lava units were partially mapped.

2. In some areas several distinct lava sequences can be identified on the basis of variable sediment cover, superposition, and relationship to regional faults. In some areas the time breaks between the emplacement of the different sequences can be no more than a few tens of years.

3. The most common lava morphology observed in all study areas is lobate lava. Sheet lavas are also moderately abundant, making up the majority of some flows, and are especially common in lava channels and within axial collapse troughs. Pillow lavas commonly form at the distal ends of several eruptive fissures and on the lateral edges of most flows; pillows make up the entire eruptive sequence in some smaller units.

4. Most individual eruptive sequences show only a limited range of major element compositional variation, which, in general, is less than those from intermediate spreading areas. However, one unit is distinctly bimodal in composition, and another shows an along-axis pattern of variability. These examples provide evidence that separate, or laterally variable, subaxial magma reservoirs can be tapped in single, or closely spaced, eruptions.

5. Volcanic eruptions are commonly not chemically unique in this area. In several cases we have identified clearly older volcanic units that have a major element chemical composition identical to younger lavas. This result indicates that the timescales of eruption must be shorter than the timescales over which the subaxial magma reservoirs are changing composition, either from significant differentiation or by variable melting processes in the underlying mantle. It also indicates that chemical mapping cannot be used to unambiguously identify the products of individual eruptions, at least in this area.

6. A comparison of our observations with those from other ridge areas suggests that there is a spreading rate dependence to the median eruptive volume, the fissure lengths activated during individual eruptions, and the chemical heterogeneity of the erupted products. Those occurring at superfast spreading have the lowest median volumes, the longest fissures, and the least chemical heterogeneity. These relationships are in accord with considerations of ridge thermal structure.

7. Available evidence suggests that eruption frequency increases with spreading rate, and hence the period between eruptions decreases. Thus volcanic activity at superfast spreading ridges tends to be much less episodic than at slower spreading ridges.

[50] **Acknowledgments.** Captain George Silva and the crew of R/V *Atlantis* cruise 3–31 provided an extremely efficient and congenial atmosphere at sea. Dudley Foster and the *Alvin* pilots are thanked for their many amazing feats of dexterity with submersible operations. Matt Naiman supervised the DSL 120 operations at sea. The overall success of cruise AT3-31 largely reflects the careful precruise planning directed by Andy Bowen and Dan Fornari of Woods Hole Oceanographic Institution. Dive observations by Mario Aigner-Torres, Milene Cormier, Bill Ryan, Anjana Shah, and Cindy Lee Van Dover contributed to our interpretations. We thank Rachel Haymon for prepublication use of DSL-120 and ARGO II imagery from the Sojourn Expedition in planning our work. This manuscript has benefited from careful reviews by Garrett Ito, Peter Michael, Matt Smith, Emily Klein, and an anonymous reviewer. Many figures used in this paper were prepared using the GMT software package [*Wessel and Smith*, 1998]. This research was supported by NSF grants OCE96-33398 and OCE98-11276. This is SOEST contribution 5872.

References

Auzende, J.-M., J. Sinton and Scientific Party, NAUDUR explorers discover recent volcanic activity along the East Pacific Rise, *Eos Trans. AGU*, *75*, 601, 604–605, 1994.

Auzende, J.-M., V. Ballu, R. Batiza, D. Bideau, J. L. Charlou, M. H. Cormier, Y. Fouquet, P. Geistdorfer, Y. Lagabrielle, J. Sinton, and P. Spadea, Recent tectonic, magmatic, and hydrothermal activity on the East Pacific Rise between 17° and 19°S: Submersible observations, *J. Geophys. Res.*, *101*, 17,995–18,010, 1996.

Ballard, R. D., and T. H. van Andel, Morphology and tectonics of the inner rift valley at lat 36°50′N on the Mid-Atlantic Ridge, *Geol. Soc. Am. Bull.*, *88*, 507–530, 1977.

Batiza, R., et al., Petrology, chemistry and petrogenesis of Leg 142 basalts - synthesis of results, *Proc. Ocean Drill. Program Sci. Results*, *142*, 3–8, 1995.

Batiza, R., Y. Niu, J. L. Karsten, W. Boger, E. Potts, L. Norby, and R. Butler, Steady and non-steady state magma chambers below the East Pacific Rise, *Geophys. Res. Lett.*, *23*, 221–224, 1996.

Bergmanis, E. C., J. M. Sinton, S. White, K. Macdonal, R. Batiza, K. Rubin, T. K. P. Gregg, C. Van Dover, and K. Grönvold, Anatomy of a mid-ocean ridge volcanic eruption: The Aldo-Kihi flow between 17°24′S and 17°34′S, East Pacific Rise, *Eos Trans. AGU*, *80*(46), Fall Meet. Suppl., F1075, 1999.

Bjornsson, A., Dynamics of crustal rifting in NE Iceland, *J. Geophys. Res.*, *90*, 10,151–10,162, 1985.

Bryan, W. B., and J. G. Moore, Compositional variations of young basalts in the Mid-Atlantic Ridge rift valley near 36°49′N, *Geol. Soc. Am. Bull.*, *88*, 556–570, 1977.

Buck, W. R., S. M. Carbotte, and C. Mutter, Controls on extrusion at mid-ocean ridges, *Geology*, *25*, 935–938, 1997.

Carlut, J., and D. V. Kent, Paleointensity record in zero-age submarine basalt glass: Testing a new dating technique for recent MORBs, *Earth Planet. Sci. Lett.*, *183*, 389–401, 2000.

Chadwick, W. W., Jr., and R. W. Embley, Lava flows from a mid-1980s submarine eruption on the Cleft Segment, Juan de Fuca Ridge, *J. Geophys. Res.*, *99*, 4761–4776, 1994.

Chadwick, W. W., Jr., R. W. Embley, and C. G. Fox, Evidence for volcanic eruption on the southern Juan de Fuca Ridge between 1981 and 1987, *Nature*, *350*, 416–418, 1991.

Chadwick, W. W., Jr., R. W. Embley, and C. G. Fox, SeaBeam depth changes associated with recent lava flows, CoAxial segment, Juan de Fuca Ridge: Evidence for multiple eruptions between 1981–1993, *Geophys. Res. Lett.*, *22*, 167–170, 1995.

Chadwick, W. W., Jr., R. W. Embley, and T. M. Shank, The 1996 Gorda Ridge eruption: Geologic mapping, sidescan sonar, and SeaBeam comparison results, *Deep Sea Res., Part II*, *45*, 2547–2569, 1998.

Chadwick, W. W., Jr., T. K. P. Gregg, and R. W. Embley, Submarine lineated sheet flows: A unique lava morphology formed on subsiding lava ponds, *Bull. Volcanol.*, *61*, 194–206, 1999.

Crane, K., and R. D. Ballard, Volcanics and structure of the Famous-Narrowgate Rift: Evidence for cyclic evolution: AMAR 1, *J. Geophys. Res.*, *86*, 5112–5124, 1981.

Dekov, V. M., and V. M. Kuptsov, Rates of accumulation of metal-bearing sediments on the East Pacific Rise (20°S), *Oceanology*, *30*, 321–324, 1990.

Dekov, V. M., and V. M. Kuptsov, Late Quaternary rates of accumulation of metal-bearing sediments on the East Pacific Rise, *Oceanology*, *32*, 94–101, 1994.

Detrick, R. S., A. J. Harding, G. M. Kent, J. A. Orcutt, J. C. Mutter, and P. Buhl, Seismic structure of the southern East Pacific Rise, *Science*, *259*, 499–503, 1993.

Dziak, R. P., C. G. Fox, and A. E. Schreiner, The June-July 1993 seismoacoustic event at CoAxial segment, Juan de Fuca Ridge: Evidence for a lateral dike injection, *Geophys. Res. Lett.*, *22*, 135–138, 1995.

Edwards, M. H., G. J. Kurras, D. R. Bohnenstiehl, B. J. Coakley, and J. R. Cochran, Evidence of recent volcanic activity on the ultraslow-spreading Gakkel Ridge, *Nature*, *409*, 808–812, 2001.

Einarsson, P., The Krafla rifting episode 1975–1989, in *The Nature of Lake Mývatn (in Icelandic)*, edited by A. Gardarson and Á. Einarsson, pp. 9–139, Icelandic Nat. Sci. Soc., Reykjavík, 1991.

Einarsson, P., and B. Brandsdottir, Seismological evidence for lateral magma intrusion during the July 1978 deflation of the Krafla volcano in NE-Iceland, *J. Geophys.*, *47*, 160–165, 1980.

Embley, R.W., and W.W. Chadwick Jr., Volcanic and hydrothermal processes associated with a recent phase of seafloor spreading at the northern Cleft segment: Juan de Fuca Ridge, *J. Geophys. Res.*, *99*, 4741–4760, 1994.

Embley, R. W., W. W. Chadwick Jr., M. R. Perfit, and E. T. Baker, Geology of the north Cleft segment, Juan de Fuca Ridge: Recent lava flows, seafloor spreading, and the formation of megaplumes, *Geology*, *19*, 771–775, 1991.

Embley, R. W., J. E. Lupton, G. Massoth, T. Urabe, V. Tunnicliffe, D. A. Butterfield, T. Shibata, O. Okano, M. Kinoshita, and K. Fujioka, Geological, chemical, and biological evidence for recent volcanism at 17.5°S: East Pacific Rise, *Earth Planet. Sci. Lett.*, *163*, 131–147, 1998.

Embley, R. W., W. W. Chadwick Jr., M. R. Perfit, M. C. Smith, and J. R. Delaney, Recent eruptions on the CoAxial segment of the Juan de Fuca Ridge: Implications for mid-ocean ridge accretion processes, *J. Geophys. Res.*, *105*, 16,501–16,526, 2000.

Fouquet, Y., J. M. Auzende, B. Ballu, R. Batiza, D. Bideau, M. H. Cormier, P. Geistdorfer, Y. Lagabrielle, J. Sinton, and P. Spadea, Hydrothermalisme et sulferes sur la dorsale du Pacifique est entre 17° et 19°S (campagne NAUDUR), *C. R. Acad. Sci., Ser. II*, *319*, 1399–1406, 1994.

Fox, C. G., R. P. Dziak, H. Matsumoto, and A. E. Schreiner, Potential for monitoring low-level seismicity on the Juan de Fuca Ridge using military hydrophone arrays, *J. Mar. Technol. Soc.*, *27*, 22–30, 1994.

Ghiorso, M. S., and R. O. Sack, Chemical mass transfer in magmatic processes, IV, A revised and internally consistent thermodynamic model for the interpretation and extrapolation of liquid-solid equilibria in magmatic systems at elevated temperatures and pressures, *Contrib. Mineral. Petrol.*, *119*, 197–212, 1995.

Gregg, T. K. P., and J. H. Fink, Quantification of submarine lava flow morphology through analog experiments, *Geology*, *23*, 73–76, 1995.

Gregg, T. K. P., and D. J. Fornari, Long submarine lava flows: observations and results from numerical modeling, *J. Geophys. Res.*, *103*, 27,517–27,532, 1998.

Gregg, T. K. P., D. J. Fornari, M. R. Perfit, R. M. Haymon, and J. H. Fink, Rapid emplacement of a mid-ocean ridge lava flow on the East Pacific Rise at 9°46′–51′N, *Earth Planet. Sci. Lett.*, *144*, E1–E7, 1996.

Grönvold, K., Mývatn fires 1724–1729, chemical composition of the lava, *Nord. Volcanol. Inst. Rep.*, *84–01*, 30 pp., 1984.

Grönvold, K., and H. Mäkkipä, Chemical composition of Krafla lavas 1975–1977, *Nord. Volcanol. Inst. Rep.*, *78-16*, 49 pp., 1978.

Gundmundsson, A. T., Volcanoes in Iceland, 136 pp., Vaka-Helgafell, Reykjavik, 1996.

Hall, L. H., and J. M. Sinton, Geochemistry of the large near-axis lava flow, East Pacific Rise near 8°S, *Earth Planet. Sci. Lett.*, *142*, 241–252, 1996.

Harris, A. J. L., J. B. Murray, S. E. Aries, M. A. Davies, L. P. Flynn, M. J. Wooster, R. Wright, and D. A. Rothery, Effusion rate trends at Etna and Krafla and their implications for eruptive mechanisms, *J. Volcanol. Geotherm. Res.*, *102*, 237–270, 2000.

Haymon, R. M., et al., Volcanic eruption of the mid-ocean ridge along the East Pacific Rise crest at 9°45–52′N: Direct submersible observations of seafloor phenomena associated with an eruption event in April, 1991, *Earth Planet. Sci. Lett.*, *119*, 85–101, 1993.

Haymon, R. M., et al., Distribution of fine-scale hydrothermal, volcanic and tectonic features along the EPR crest, 17°15′–18°30′S: Results of near-bottom acoustic and optical surveys, *Eos Trans. AGU*, *78*(46), Fall Meet. Suppl. F705, 1997.

Head, J. W., III, L. Wilson, and D. K. Smith, Mid-ocean ridge eruptive vent morphology and substructure, *J. Geophys. Res.*, *101*, 28,265–28,280, 1996.

Hekinian, R., J. G. Moore, and W. B. Bryan, Volcanic rocks and processes of the Mid-Atlantic Ridge rift valley near 36°49′N, *Contrib. Mineral. Petrol.*, *58*, 83–110, 1976.

Hooft, E. E. E., and R. S. Detrick, The role of density in the accumulation and eruptibility of basaltic melts at mid-ocean ridges, *Geophys. Res. Lett.*, *20*, 423–426, 1993.

Hooft, E. E. E., R. S. Detrick, and G. M. Kent, Seismic structures and indicators of magma budget along the southern East Pacific Rise, *J. Geophys. Res.*, *102*, 27,319–27,340, 1997.

Lagabrielle, Y., and M.-H. Cormier, Formation of large summit troughs along the East Pacific Rise as collapse calderas: An evolutionary model, *J. Geophys. Res.*, *104*, 12,971–12,988, 1999.

Lawson, K. R. C. Searle, J. A. Pearce, P. Browning, and P. Kempton, Detailed volcanic geology of the MARNOK area, Mid-Atlantic Ridge, north of Kane transform, in *Tectonic, Magmatic, Hydrothermal and Biological Segmentation of Mid-Ocean Ridges*, edited by C. J. MacLeod, P. A. Tyler, and C. L. Walker, *Geol. Soc. Spec. Publ.*, *118*, 6–102, 1996.

Luyendyck, B. P., and K. C. Macdonald, Physiography and structure of the Famous Rift Valley inner floor observed with a deep towed instrument package, *Geol. Soc. Am. Bull.*, *88*, 621–636, 1977.

Lyle, M., M. Leinen, R. M. Owen, and D. K. Rea, Late Tertiary history of hydrothermal deposition at the East Pacific Rise, 19°S, *Geophys. Res. Lett.*, *14*, 595–598, 1987.

Macdonald, K. C., Linkages between faulting, volcanism, hydrothermal activity and segmentation on fast-spreading centers, in *Faulting and Magmatism at Mid-Ocean Ridges, Geophys. Monogr. Ser.*, vol. 106, edited by W. R. Buck et al., pp. 27–58, AGU, Washington, D. C., 1998.

Macdonald, K. C., and P. J. Fox, The axial summit graben and cross-sectional shape of the East Pacific Rise as indicators of axial magma chambers and recent volcanic eruptions, *Earth Planet. Sci. Lett.*, *88*, 119–131, 1988.

Macdonald, K. C., R. Haymon, and A. Shor, A 220 km2 recently erupted lava field on the East Pacific Rise near lat 8°S, *Geology*, *17*, 212–216, 1989.

Marchig, V. J. Erzinger, and P.-M. Heinze, Sediment in the black smoker area of the East Pacific Rise (18.5°S), *Earth Planet. Sci. Lett.*, *79*, 93–106, 1986.

MELT Seismic Team, Imaging the deep seismic structure beneath a mid-ocean ridge: The MELT experiment, *Science*, *280*, 1215–1218, 1998.

Mutter, J. C., S. M. Carbotte, W. Su, L. Xu, P. Buhl, R. S. Detrick, G. M. Kent, J. A. Orcutt, and A. J. Harding, Seismic images of active magma systems beneath the East Pacific Rise between 17°05′ and 17°35′S, *Science*, *268*, 391–395, 1995.

Naar, D. F., and R. N. Hey, Recent Pacific-Easter-Nazca plate motions, in *Evolution of Mid-Ocean Ridges, Geophys. Monogr. Ser.*, vol. 57, edited by J. M Sinton, pp. 9–30, AGU, Washington, D. C., 1989.

Perfit, M. R., and W. W. Chadwick Jr., Magmatism at mid-ocean ridges: Constraints from volcanological and geochemical investigations, in *Faulting and Magmatism at Mid-Ocean Ridges*, *Geophys. Monogr. Ser.*, vol. 106, edited by W. R. Buck et al., pp. 59–115, AGU, Washington, D. C., 1998.

Perfit, M. R., D. J. Fornari, M. C. Smith, J. F. Bender, C. H. Langmuir, and R. M. Haymon, Small-scale spatial and temporal variations in mid-ocean ridge crest magmatic processes, *Geology*, *22*, 375–379, 1994.

Reynolds, J. A., C. H. Langmuir, J. F. Bender, K. A. Kastens, and W. B. F. Ryan, Spatial and temporal variability in the geochemistry of basalts from the East Pacific Rise, *Nature*, *359*, 493–499, 1992.

Rhodes, J. M., Homogeneity of lava flows: Chemical data for historic Mauna Loa eruptions, *Proc. Lunar Planet. Sci. Conf. 13th, Part 2, J. Geophys. Res.*, *88*, suppl., A869–A879, 1983.

Rowland, S. K., and G. P. L. Walker, Toothpaste lava: characteristics and origin of a lava sturctural type transitional between pahoehoe and aa, *Bull. Volcanol.*, *49*, 631–641, 1987.

Rubin, A. M., Tensile fracture of rock at high confining pressure: Implications for dike propagation, *J. Geophys. Res.*, *98*, 15,919–15,935, 1993.

Rubin, K. H., J. D. Macdougall, and M. R. Perfit, ^{210}Po–^{210}Pb dating of recent volcanic eruptions on the sea floor, *Nature*, *368*, 841–844, 1994.

Rubin, K. H., M. C. Smith, M. R. Perfit, D. M. Christie, and L. F. Sacks, Geochronology and petrology of lavas from the 1996 North Gorda Ridge eruption, *Deep Sea Res., Part II*, *45*, 2571–2597, 1998.

Rubin, K. H., M. D. Smith, E. C. Bergmanis, M. R. Perfit, J. M. Sinton, and R. Batiza, Magmatic history and volcanological insights from individual lava flows erupted on the seafloor, *Earth Planet. Sci. Lett.*, *188*, 349–367, 2001.

Saemundsson, K., Jardfraedi Kröflukerfisins, in *The Nature of Lake Mývatn* (in Icelandic), edited by A. Gardarson and Á. Einarsson, pp. 2–95, Icelandic Nat. Sci. Soc., Reykjavík, 1991.

Saemundsson, K., Geology of the Thinvallavatn area, *Oikos*, *64*, 40–68, 1992.

Scheirer, D. S., and K. C. Macdonald, Variation in cross-sectional area of the axial ridge along the East Pacific Rise: Evidence for the magmatic budget of a fast spreading center, *J. Geophys. Res.*, *98*, 7871–7885, 1993.

Scheirer, D. S., et al., A map series of the southern East Pacific Rise and its flanks, 15° to 19°S, *Mar. Geophys. Res.*, *18*, 1–12, 1996.

Shibata, T., O. Okano, R. W. Embley, K. Nogami, K. Fujioka, K. Sayanagi, and M. Kinoshita, Along-axis fractionation of basalts: Samples from the recent lava flows at 17° 24-35′S, East Pacific Rise, *Eos Trans. AGU*, *80*(46), Fall Meet. Suppl., F1075, 1999.

Sinton, J. M., Eruptive history of the Hengill Volcanic System: Mid-Atlantic Ridge in the Western Volcanic Zone of Iceland, *Eos Trans. AGU*, *78*(46), Fall Meet. Suppl., F645, 1997a.

Sinton, J. M., Spreading rate dependence to volcanic eruptions on mid-ocean ridges: Speculations from observations, reservoirs constraints and ridge structure, *Eos Trans. AGU*, *78*(46), Fall Meet. Suppl., F663, 1997b.

Sinton, J. M., and R. S. Detrick, Mid-ocean ridge magma chambers, *J. Geophys. Res.*, *97*, 197–216, 1992.

Sinton, J. M., S. M. Smaglik, J. J. Mahoney, and K. C. Macdonald, Magmatic processes at superfast spreading mid-ocean ridges: Glass compositional variations along the East Pacific Rise, 13°-23°S, *J. Geophys. Res.*, *96*, 6133–6155, 1991.

Sinton, J. M., et al., Volcanological investigations at superfast spreading: Results from R/V *Atlantis* cruise 3-31, *RIDGE Events*, *10*, 17–23, 1999.

Smith, D. K., and J. R. Cann, Hundreds of small volcanoes on the median valley floor of the Mid-Atlantic Ridge (24°–30° N), *Nature*, *348*, 152–155, 1990.

Smith, D. K., and J. R. Cann, The role of seamount volcanism in crustal construction at the Mid-Atlantic Ridge (24°–30°N), *J. Geophys. Res.*, *97*, 1645–1658, 1992.

Smith, M. D., Geochemistry of eastern Pacific MORB: Implications for

MORB petrogenesis and the nature of crustal accretion within the neovolcanic zones of two recently active ridge segments, Ph.D. thesis, Univ. of Fla., Gainsville, 1999.

Smith, M. C., M. R. Perfit, and I. R. Jonasson, Petrology and geochemistry of basalts from the southern Juan de Fuca Ridge: Controls on the spatial and temporal evolution of mid-ocean ridge basalt, *J. Geophys. Res.*, *99*, 4787–4812, 1994.

Stakes, D. S., J. W. Shervais, and C. A. Hopson, The volcanic-tectonic cycle of the FAMOUS and AMAR valleys, Mid-Atlantic Ridge (36°47′N): Evidence from basalt glass and phenocryst compositional variations for a steady-state magma chamber beneath the valley midsections, AMAR 3, *J. Geophys. Res.*, *89*, 6995–7028, 1984.

Tryggvason, E., Widening of the Krafla fissure swarm during the 1975-1981 volcano-tectonic episode, *Bull. Volcanol.*, *47*, 47–69, 1984.

Tryggvason, E., Multiple magma reservoirs in a rift zone volcano: Ground deformation and magma transport during the September eruption of Krafla, Iceland, *J. Volcanol. Geotherm. Res.*, *28*, 1–44, 1986.

Urabe, T., et al., The effect of magmatic activity on hyrothermal venting along the superfast spreading East Pacific Rise, *Science*, *269*, 1092–1095, 1995.

Wessel, P., and W. H. F. Smith, New, improved version of the Generic Mapping Tools released, *Eos Trans. AGU*, *79*, 579, 1998.

White, S. M., K. C. Macdonald, and R. M. Haymon, Basaltic lava domes, lava lakes, and volcanic segmentation on the southern East Pacific Rise, *J. Geophys. Res.*, *105,* 23,519–23,536, 2000.

R. Batiza, National Science Foundation, Division of Ocean Sciences, 4201 Wilson Blvd., Arlington, VA 22230, USA. (rbatiza@nsf.gov)

E. Bergmanis, K. Rubin, and J. Sinton, Department of Geology and Geophysics, University of Hawaii, 2525 Correa Road, Honolulu, HI 96822, USA. (ericb@soest.hawaii.edu; krubin@soest.hawaii.edu; sinton@soest.hawaii.edu)

T. K. P. Gregg, Department of Geological Sciences, 876 Natural Sciences Complex, University at Buffalo, Buffalo, NY 14260-3050, USA. (tgregg@nsm.buffalo.edu)

K. Grönvold, Nordic Volcanological Institute, 50 Grensásvegur, 108 Reykjavík, Iceland. (karl@norvol.hi.is)

K. C. Macdonald, Department of Geological Sciences, Webb Hall, Room 1006, University of California, Santa Barbara, CA 93106, USA. (macdonald@geol.ucsb.edu)

S. M. White, Department of Geological Sciences, University of South Carolina, 701 Sumter Street, Columbia, SC 29208, USA. (swhite@sc.edu)

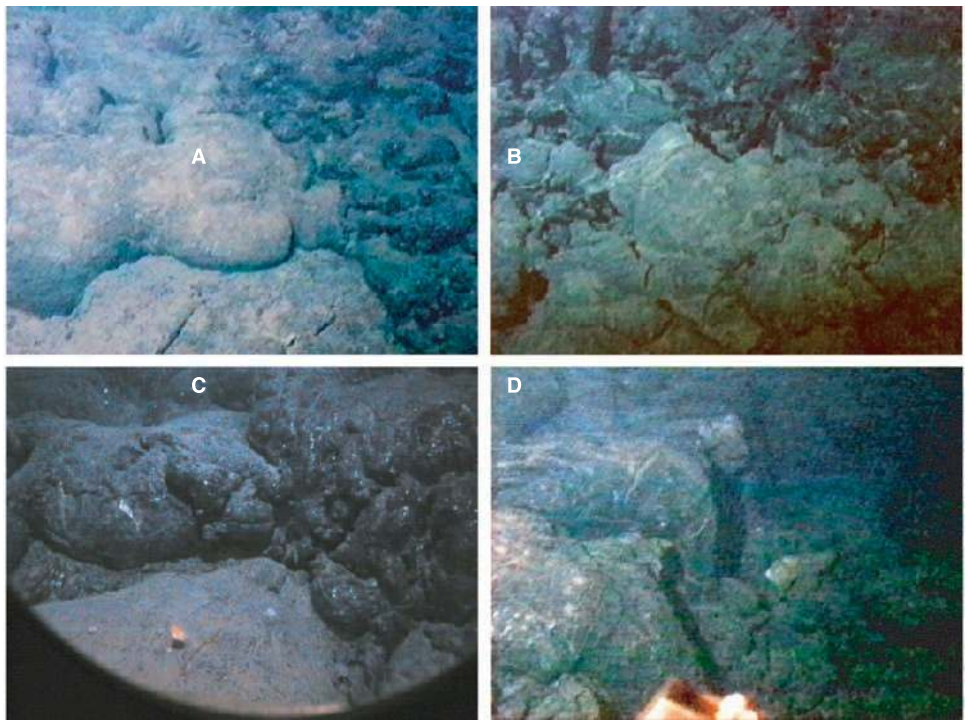

Figure 13. Photos showing a range of contact relations of the Aldo-Kihi lava flow field. Figures 13a and 13b show contacts along the western boundary of the Aldo-Kihi lava, where relatively unsedimented, slightly pillowed Aldo-Kihi lava overlies older lobate lavas with similar major element composition. (a) *Alvin* dive 3357, 17°27.83′S, 113°13.43′W; Aldo-Kihi lava on right side. (b) *Alvin* dive 3364, 17°27.03′S, 113°13.32′W; Aldo-Kihi lava on top. Figures 13c and 13d show internal contacts within the Aldo Kihi lava flow field. (c) Internal contact showing the latest phase of pillow lava overlying slightly earlier Aldo-Kihi lobate lava flow, now partially covered by hydrothermal sediment and an anemone; *Alvin* dive 3365, 17° 25.91′S, 113°12.31′W. (d) Latest Aldo-Kihi lava spilling into recent collapse pit within slightly older Aldo-Kihi lava; *Alvin* dive 3360, 17° 29.13′S, 113°13.13′W. Horizontal dimensions of Figures 13a, 13b, and 13d are ∼5 m; horizontal dimension of Figure 13c, taken through the *Alvin* pilot's view port, is ∼3 m.